IEEE Access
Multidisciplinary | Rapid Review | Open Access Journal

Received November 13, 2019, accepted November 26, 2019, date of publication December 2, 2019,
date of current version December 18, 2019.

Digital Object Identifier 10.1109/ACCESS.2019.2957036

Barrier Lyapunov Function-Based Sliding Mode Control for BWB Aircraft With Mismatched Disturbances and Output Constraints

ZHIRUN CHEN[1], QING LI[1], XIAOZHE JU[2], AND FEI CEN[1,3]
[1]Department of Automation, Tsinghua University, Beijing 100084, China
[2]School of Astronautics, Harbin Institute of Technology, Harbin 150001, China
[3]Low Speed Aerodynamic Institute, China Aerodynamic Research and Development Center, Mianyang 621000, China

Corresponding author: Qing Li (liqing@tsinghua.edu.cn)

This work was supported in part by the National Natural Science Foundation of China under Grant 61771281, in part by the New Generation Artificial Intelligence major Project of China under Grant 2018AAA0101605, in part by the 2018 Industrial Internet Innovation and Development Project, and in part by the Tsinghua University Initiative Scientific Research Program.

ABSTRACT This paper presents a barrier Lyapunov function based nonsingular fast terminal sliding mode control with fixed-time non-recursive disturbance observer for the blended-wing-body (BWB) aircraft in the presence of mismatched disturbances and output constraints. The fixed-time non-recursive disturbance observer based nonsingular fast terminal sliding mode control is proposed for matched and mismatched disturbances attenuation. Furthermore, in order to pursue high-precision attitude tracking regarded as output tracking errors constraints before disturbance observer tracking errors converge to a small prescribed range, the barrier Lyapunov function is designed to constrain the sliding mode variables before states reach the sliding mode surface. Consequently outputs tracking errors constraints can be satisfied by the sliding variables constraints. More importantly, barrier Lyapunov function based terminal sliding mode controller ensures the finite-time convergence. Finally, the numerical simulations demonstrate the chattering attenuation and high-precision attitude tracking of the BWB aircraft in the presence of mismatched disturbances and output constraints.

INDEX TERMS Barrier Lyapunov function, blended-wing-body aircraft, fixed-time non-recursive disturbance observer, mismatched disturbances, output constraints.

I. INTRODUCTION

Recent years have witnessed the extensive researches of Blended-Wing-Body (BWB) aircraft, for its advantages in stealth, aerodynamics, and structural strength. However, in contrast with traditional aircraft, BWB aircraft also causes directional static instability, low pitch damping, strong longitudinal and lateral coupling [1]–[3]. In addition, the system uncertainties including unmodeled dynamics and external disturbances further increase the pressure of BWB aircraft control system. These properties bring some critical challenges to BWB aircraft high-precision attitude tracking, which will be regarded as output tracking error constraints in the following parts.

To solve these challenges, advanced nonlinear control methods of the BWB aircraft attitude tracking have been gradually proposed. One attractive BWB aircraft control method is the sliding model control method for its robustness to the uncertainties. In particular, the terminal sliding mode control is capable of driving the aircraft attitude to desired states in finite-time [4], while the inherent singularity in terminal sliding mode control prevents its practical applications. Feng *et al.* [5] proposed the nonsingular terminal sliding mode control to avoid this problem. The nonsingular fast terminal sliding mode control approach proposed by Yang and Yang [6] achieves faster convergence, but this method's settling time depends on the initial error states of fight vehicle attitude. Such dependence is relaxed with the method of fixed-time convergence by Polyakov [7]. Recently, integral terminal sliding mode control [29], [30] for its less chattering effect contrast to conventional terminal sliding mode control methods attracts much attention. However, aforementioned sliding mode control (SMC) methods are

The associate editor coordinating the review of this manuscript and approving it for publication was Yan-Jun Liu.

only insensitive to the matched disturbance, furthermore, these methods cannot avoid chattering problem.

The mismatched disturbance is still the main control challenge in BWB aircraft high-precision control, which can also be identified in various control scenarios. Some more effective methods are studied to tackle this challenge. The traditional control methods combined with SMC have been gradually established for the mismatched disturbances, such as the LMI-based control [8], the Riccati approach [9], the adaptive control [10] Apart from integration way, integral sliding mode control [11] adopts the high frequency switching gain for the mismatched disturbances. However, these methods handle the mismatched disturbances at the cost of sacrificing its nominal control performance.

Recently, the disturbance observer (DO) based sliding mode control have been gradually developed, since the disturbance observer can reduce the magnitude of the discontinuous coefficient which can mitigate the chattering problem and recovery the nominal control performance. Different disturbance observer, such as the nonlinear-DO [12], extended DO [13], finite-time robust exact DO [14], and uniform robust exact DO [15], fixed-time DO [16], have the possibility of integrating with the different sliding mode control to handle the mismatched disturbances. Yang [17]–[19] proposes a novel continuous NTSM with the finite-time disturbance observer and nonlinear disturbance observer for systems with mismatched disturbance, which can realize the fine nominal control performance and chattering alleviation. Ginoya [15] proposes the extended disturbance observer and modifies the sliding surface for general n^{th} order system with mismatched disturbance. Zhang *et al.* [20] develops the disturbance observer based integral SMC for linear systems with mismatched disturbance. Nowadays, the DO based SMC method for mismatched disturbance have been gradually applied in unmanned helicopter [21], reusable launch vehicles [22], MAGLEV suspension vehicles areas and so on.

However, the disturbance observer based sliding mode control method cannot guarantee high-precision attitude tracking regarded as the output constraints before the disturbance observer tracking errors converge to a small prescribed range. The output constraints problem can be regarded as a special case of states constraints problem. There exist various methods to address the states constraints problem, such as model predictive control [23], reference governors [24], barrier Lyapunov function and so on. Among these methods, the barrier Lyapunov function (BLF) is an effective method to constrain the transient performance, such as the convergence accuracy and overshoot. The BLF is first proposed by Ngo *et al.* [25] for state-constrained systems in the Brunovsky form, then Tee *et al.* [26] extends it in a strict feedback form. Later, Tee and Ge [27] also develops partial state-constrained control method. Wang *et al.* [28] proposes a novel exponential barrier Lyapunov function to address state constraints and external disturbance problem. However, the above barrier Lyapunov function methods are mainly combined with backstepping technique, and outputs can converge to an invariant set, but large control inputs are needed to guarantee that the invariant set is small enough given the requirement of high-precision tracking performance.

This paper proposes a barrier Lyapunov function based nonsingular fast terminal sliding mode control with fixed-time non-recursive disturbance observer for blended-wing-body aircraft high-precision attitude tracking with mismatched disturbance and output constraints. The main contributions of this paper are stated as follows:

1) A fixed-time non-recursive disturbance observer (FxTDO) based nonsingular fast terminal sliding mode control (NFTSMC) method is established to attenuate matched and mismatched disturbance and recovery its nominal control performance. The advantages of non-recursive FxTDO lie in that its structure are simpler than recursive FxTDO and its disturbance estimations are smoother than finite-time disturbance observer. Moreover, its disturbance estimation errors are convergent in a fixed time, independent of the initial estimation errors.
2) To pursue high-precision attitude tracking, a barrier Lyapunov function is developed to constrain sliding mode variables rather than directly constrain the outputs tracking errors before the disturbance observer tracking errors converge to a small prescribed range, and then output tracking errors constraints are satisfied by the sliding mode variables constraints. More importantly, its finite-time convergence will be guaranteed.

The remainder of this paper is arranged as follows. Section II introduces the BWB aircraft dynamic model. In Section III, the formulation of BWB aircraft attitude tracking problem is stated. In section IV, a fixed-time non-recursive disturbance observer based NFTSMC method and a barrier Lyapunov function based NFTSMC method are presented for Section III problem. Simulation results are provided in Section V followed by the conclusion in Section VI.

II. BWB AIRCRAFT DYNAMIC MODEL

The mathematical dynamic model of the BWB aircraft has been widely investigated. To the best knowledge of the author, in most literature, the force and moment coefficients in BWB aircraft dynamic model are in the form of aerodynamic derivative or polynomial fitting rather than in the form of the raw wind tunnel data. This section introduces dynamic mode with raw wind tunnel data which is more accurate. Then this mode is transformed into aerodynamic derivative form for control design and the transformation errors are regarded as external disturbances.

A. BWB AIRCRAFT OVERVIEW

The BWB aircraft (in 1:10 scale) is designed to verify the control laws based on wind tunnel free flight tests. As shown in Fig. 1, BWB aircraft's control surfaces are elevator, aileron, split rudder and thrust vector engine. Besides, onboard sensors consist of the Airdata boom, Inertial

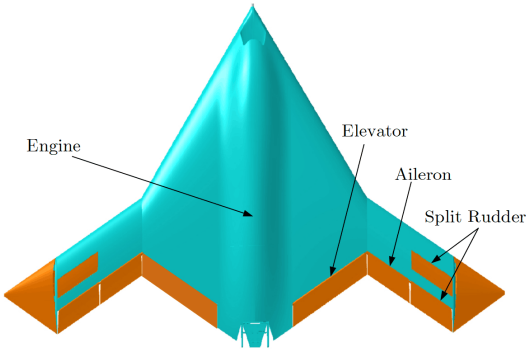

FIGURE 1. BWB aircraft configuration.

Measurement Unit (IMU), Attitude and Heading Reference System (AHRS).

B. BWB AIRCRAFT DYNAMIC MODEL

The BWB aircraft dynamic model is derived by the Newton approach. Before addressing the dynamic mode, following assumptions are presented to simplify the induction: the BWB aircraft is a rigid body; the earth's rotation and gravitational perturbation are neglected; and the wind-related terms are ignored as well. With above assumptions, the BWB aircraft attitude dynamics can be formulated as the following form:

$$\dot{\alpha} = q - \tan\beta(p\cos\alpha + r\sin\alpha) + \frac{1}{MV\cos\beta}(-L + Mg\cos\gamma\cos\mu - T_x\sin\alpha + T_z\cos\alpha) \tag{1}$$

$$\dot{\beta} = -r\cos\alpha + p\sin\alpha + \frac{1}{MV}(Y\cos\beta + Mg\cos\gamma\sin\mu) + \frac{1}{MV}(-T_x\sin\beta\cos\alpha + T_y\cos\beta - T_z\sin\alpha\sin\beta) \tag{2}$$

$$\dot{\mu} = \sec\beta(p\cos\alpha + r\sin\alpha) + \frac{L}{MV}(\tan\beta + \tan\gamma\sin\mu) + \frac{(Y+T_y)}{MV}\tan\gamma\cos\mu\cos\beta - \frac{g}{V}\cos\gamma\cos\mu\tan\beta + \frac{T_x}{MV}(\tan\gamma(\sin\mu\sin\alpha - \cos\mu\sin\beta\cos\alpha) + \tan\beta\sin\alpha) - \frac{T_z}{MV}(\tan\gamma(\sin\mu\cos\alpha + \cos\mu\sin\beta\sin\alpha) + \tan\beta\cos\alpha) \tag{3}$$

$$\dot{p} = \frac{I_z(l_{aero} + l_T) + I_{xz}(n_{aero} + n_T)}{I_xI_z - I_{xz}^2} + \frac{pqI_{xz}(I_x - I_y + I_z) + qr(I_yI_z - I_z^2 - I_{xz}^2)}{I_xI_z - I_{xz}^2} \tag{4}$$

$$\dot{q} = \frac{(m_{aero} + m_T) + (I_z - I_x)pr - I_{xz}(p^2 - r^2)}{I_y} \tag{5}$$

$$\dot{r} = \frac{I_{xz}(l_{aero} + l_T) + I_x(n_{aero} + n_T)}{I_xI_z - I_{xz}^2} + \frac{pq(I_z^2 - I_yI_z + I_{xz}^2) - qrI_{xz}(I_x - I_y + I_z)}{I_xI_z - I_{xz}^2} \tag{6}$$

where α, β, γ, μ represent angle of attack, angle of sideslip, flight path angle, and flight roll angle; p, q, r represent roll rate, pitch rate, and yaw rate; M represents mass of the BWB aircraft; I_x, I_y, I_z, I_{xz} represent rotational inertia of the x-axis, y-axis, z-axis, x-z plane; L, Y represent aerodynamic lift force and aerodynamic side force; T_x, T_y, T_z represent the x-axis, y-axis, z-axis force produced by thrust vector engine; $l_{aero}, m_{aero}, n_{aero}$ represent aerodynamic roll torque, aerodynamic pitch torque, and aerodynamic yaw torque; l_T, m_T, n_T represent roll torque, pitch torque, and yaw torque produced by thrust vector engine.

The aerodynamic forces and torques are expressed as $L = QSC_L$, $Y = QSC_Y$, $l = QSbC_l$, $m = QScC_l$, $n = QScC_n$, where Q represents dynamic pressure, S represents aerodynamic reference area. The lift force, drag force, side force, roll torque, pitch torque, and yaw torque coefficients are given as follows:

$$\begin{aligned} C_L &= C_{Lbasic}(\alpha,\beta) + \Delta C_{Lde}(\alpha,\delta_e) + \Delta C_{Lda}(\alpha,\beta,\delta_a) \\ &\quad + \Delta C_{Ldr}(\alpha,\beta,\delta_r) \\ C_D &= C_{Dbasic}(\alpha,\beta) + \Delta C_{Dde}(\alpha,\delta_e) + \Delta C_{Dda}(\alpha,\beta,\delta_a) \\ &\quad + \Delta C_{Ddr}(\alpha,\beta,\delta_r) \\ C_Y &= C_{Ybasic}(\alpha,\beta) + \Delta C_{Yda}(\alpha,\beta,\delta_a) + \Delta C_{Ydr}(\alpha,\beta,\delta_r) \end{aligned} \tag{7}$$

$$\begin{aligned} C_l &= C_{lbasic}(\alpha,\beta) + \Delta C_{lda}(\alpha,\beta,\delta_a) + \Delta C_{ldr}(\alpha,\beta,\delta_r) \\ &\quad + (pb/2V)C_{l_p}(\alpha) + (rb/2V)C_{l_r}(\alpha) \\ C_m &= C_{mbasic}(\alpha,\beta) + \Delta C_{mde}(\alpha,\delta_e) + \Delta C_{mda}(\alpha,\beta,\delta_a) \\ &\quad + \Delta C_{mdr}(\alpha,\beta,\delta_r) + (p\bar{c}/2V)C_{m_q}(\alpha) \\ C_n &= C_{nbasic}(\alpha,\beta) + \Delta C_{nda}(\alpha,\beta,\delta_a) + \Delta C_{ndr}(\alpha,\beta,\delta_r) \\ &\quad + (pb/2V)C_{n_p}(\alpha) + (rb/2V)C_{n_r}(\alpha) \end{aligned} \tag{8}$$

where $C_{Y_p}, C_{Y_r}, C_{Z_q}, C_{n_p}, C_{n_r}$ are dynamic derivative coefficients.

The forces and torques of thrust vector engine are:

$$\begin{cases} T_x = T \\ T_y = 0.75T\delta_y \\ T_z = -T\delta_z \end{cases}, \quad \begin{cases} l_T = 0 \\ m_T = X_TT_z \\ n_T = -X_TT_y \end{cases} \tag{9}$$

where T, δ_y, δ_z represent engine thrust, lateral and normal thrust vectoring control deflection angles.

The force and torque coefficients in Equ. (7) and (8) is obtained by interpolation with wind tunnel test data. However, most advanced nonlinear flight control methods are designed for affine nonlinear system, and it's difficult to adopt feedback linearization for system with interpolation. Therefore, aerodynamic derivatives form will be introduced.

C. BWB AIRCRAFT AERODYNAMIC DERIVATIVE

The weighted least squares algorithm are adopted to obtain aerodynamic derivatives, which transforms primitive system into affine nonlinear system. Equ. (7) and (8) are transformed

into the following form:

$$\begin{aligned}
C_L &= C_{Lbasic} + C_L^{\delta_e}(\alpha)\delta_e + d_{11} \\
C_Y &= C_{Ybasic} + C_Y^{\delta_r}(\alpha,\beta)\delta_r + C_Y^{\delta_a}(\alpha,\beta)\delta_a + d_{12} \\
C_D &= C_{Dbasic} + C_D^{\delta_e}(\alpha)\delta_e + d_{13} \qquad (10) \\
C_l &= C_{lbasic} + C_l^{\delta_a}(\alpha,\beta)\delta_a + C_l^{\delta_r}(\alpha,\beta)\delta_r \\
&\quad + \left(pb/2V\right) C_{l_p}(\alpha) + \left(rb/2V\right) C_{l_r}(\alpha) + d_{21} \\
C_m &= C_{mbasic} + C_m^{\delta_e}(\alpha,\beta)\delta_e + \left(p\bar{c}/2V\right) C_{m_q}(\alpha) + d_{22} \\
C_n &= C_{nbasic} + C_n^{\delta_a}(\alpha,\beta)\delta_a + C_n^{\delta_r}(\alpha,\beta)\delta_r \\
&\quad + \left(pb/2V\right) C_{n_p}(\alpha) + \left(rb/2V\right) C_{n_r}(\alpha) + d_{23} \qquad (11)
\end{aligned}$$

where $\boldsymbol{d}_{a1} = [d_{11}, d_{12}, d_{13}]^T$, $\boldsymbol{d}_{a2} = [d_{21}, d_{22}, d_{23}]^T$ are transformation errors.

III. PROBLEM FORMULATION

The attitude dynamic model in the form of aerodynamic derivatives can be rewritten as the following compact form

$$\begin{aligned}
&\begin{cases} \dot{\boldsymbol{x}}_1 = \boldsymbol{F}(\boldsymbol{x}_1, \boldsymbol{x}_2) + \boldsymbol{d}_1 \\ \dot{\boldsymbol{x}}_2 = \boldsymbol{H}(\boldsymbol{x}_1, \boldsymbol{x}_2) + \boldsymbol{G}(\boldsymbol{x}_1, \boldsymbol{x}_2)\boldsymbol{u} + \boldsymbol{d}_2 \end{cases} \\
&\boldsymbol{y} = \boldsymbol{x}_1 \qquad (12)
\end{aligned}$$

where $\boldsymbol{x}_1 = [\alpha, \beta, \mu]^T$, $\boldsymbol{x}_2 = [p, q, r]^T$, $\boldsymbol{u} = [\delta_e, \delta_a, \delta_r, \delta_y, \delta_z]^T$. $\boldsymbol{d}_1$ are mismatched disturbances, which contain $\boldsymbol{d}_{a1}$ and neglected dynamics; $\boldsymbol{d}_2$ are matched disturbances, which contain $\boldsymbol{d}_{a2}$ and external disturbances; $F(\boldsymbol{x}_1, \boldsymbol{x}_2)$, $\boldsymbol{H}(\boldsymbol{x}_1, \boldsymbol{x}_2)$, $\boldsymbol{G}(\boldsymbol{x}_1, \boldsymbol{x}_2)$ are continuous vector functions, expressed as:

$$\boldsymbol{F}(\boldsymbol{x}_1, \boldsymbol{x}_2) = \begin{bmatrix} -\tan\beta\cos\alpha & 1 & -\tan\beta\sin\alpha \\ \sin\alpha & 0 & -\cos\alpha \\ \sec\beta\cos\alpha & 0 & \sec\beta\sin\alpha \end{bmatrix} \begin{bmatrix} p \\ q \\ r \end{bmatrix},$$

$$\boldsymbol{H}(\boldsymbol{x}_1, \boldsymbol{x}_2) = \boldsymbol{J}^{-1} \left(-\boldsymbol{x}_2^{\times}\boldsymbol{J}\boldsymbol{x}_2 + \begin{bmatrix} QSb(C_{lbasic} + \frac{pb}{2V}C_{l_p} + \frac{rb}{2V}C_{l_r}) \\ QSc(C_{mbasic}\frac{qc}{2V}C_{m_q}) \\ QSb(C_{nbasic} + \frac{pb}{2V}C_{n_p} + \frac{rb}{2V}C_{n_r}) \end{bmatrix} \right)$$

$$\boldsymbol{G}(\boldsymbol{x}_1, \boldsymbol{x}_2) = \boldsymbol{J}^{-1}\boldsymbol{W},$$

where $\boldsymbol{J} = \begin{bmatrix} J_x & 0 & J_{xz} \\ 0 & J_y & 0 \\ J_{xz} & 0 & J_z \end{bmatrix}$,

$$\boldsymbol{W} = \begin{bmatrix} 0 & QSbC_l^{\delta_a} & QSbC_l^{\delta_r} & 0 & 0 \\ QScC_m^{\delta_e} & QScC_m^{\delta_a} & 0 & 0 & -X_T T \\ 0 & QSbC_n^{\delta_a} & QSbC_n^{\delta_r} & -0.75X_T T & 0 \end{bmatrix}.$$

Transforming the equation (12) into the following form:

$$\begin{cases} \dot{\boldsymbol{\varepsilon}} = \boldsymbol{F}(\boldsymbol{x}_1, \boldsymbol{x}_2) - \dot{\boldsymbol{x}}_d + \boldsymbol{d}_1 \\ \dot{\boldsymbol{x}}_2 = \boldsymbol{H}(\boldsymbol{x}_1, \boldsymbol{x}_2) + \boldsymbol{G}(\boldsymbol{x}_1, \boldsymbol{x}_2)\boldsymbol{u} + \boldsymbol{d}_2 \end{cases} \qquad (13)$$

where $\boldsymbol{\varepsilon} = \boldsymbol{x}_1 - \boldsymbol{x}_d$ represent tracking errors.

In this paper, our ultimate aim is to develop a control algorithm such that $\boldsymbol{x}_1$ can track the given commands $\boldsymbol{x}_d$ in finite-time in the presence of mismatched disturbances and output constraints.

IV. CONTROL DESIGN

To pursue high-precision attitude tracking of BWB attitude, a novel composite nonsingular fast terminal sliding mode control, combining with barrier Lyapunov function and fixed-time non-recursive disturbance observer, is proposed. The fixed-time non-recursive disturbance observer is constructed to estimate matched disturbance and mismatched disturbance simultaneously for chattering attenuation, which results in the reduction of the switching gains. To accelerate the convergence rate, a novel nonsingular fast terminal sliding mode surface is constructed. Besides, considering the output tracking errors constraints, the barrier Lyapunov function is developed to constrain the sliding mode variables, further satisfy output tracking errors constraints. The BWB aircraft high-precision attitude tracking control scheme is shown in Fig. 2.

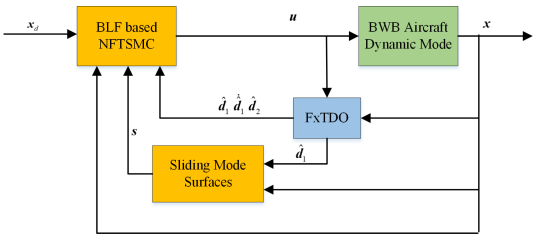

FIGURE 2. BWB aircraft control scheme.

In the following part, the FxTDO based NFTSMC will be firstly introduced followed by the barrier Lyapunov function based NFTSMC.

A. FxTDO DESIGN

Considering the system dynamic (13), a fixed-time non-recursive disturbance observer (FxTDO) is proposed to estimate $\boldsymbol{d}_1$ and $\boldsymbol{d}_2$ simultaneously, which is inspired by [16]. Moreover it can be divided into two sub-observers. Considering practical properties of the BWB aircraft disturbances, following assumption is presented.

Assumption 1 [31]: Considering the engineering practice of the BWB aircraft disturbances, there exist a small enough constant ρ and the fixed-time non-recursive disturbance observer orders $l_1 = 3, l_2 = 2$ such that $\left\|\boldsymbol{d}_1^{(l_1-1)}\right\| \le \rho$, $\left\|\boldsymbol{d}_2^{(l_2-1)}\right\| \le \rho$.

Then a FxTDO is adopted to estimate $\boldsymbol{d}_1$ and $\dot{\boldsymbol{d}}_1$, the concrete form is shown as follows:

$$\begin{aligned}
\dot{\hat{\boldsymbol{\varepsilon}}} &= \boldsymbol{F}(\boldsymbol{x}_1, \boldsymbol{x}_2) - \dot{\boldsymbol{x}}_d + \boldsymbol{v}_0 \\
\boldsymbol{v}_0 &= -k_{10}\left|\hat{\boldsymbol{\varepsilon}} - \boldsymbol{\varepsilon}\right|^{\alpha_1} \circ sgn(\hat{\boldsymbol{\varepsilon}} - \boldsymbol{\varepsilon}) \\
&\quad - \kappa_{10}\left|\hat{\boldsymbol{\varepsilon}} - \boldsymbol{\varepsilon}\right|^{\beta_1} \circ sgn(\hat{\boldsymbol{\varepsilon}} - \boldsymbol{\varepsilon}) + \boldsymbol{\varepsilon}_1 \\
\dot{\boldsymbol{\varepsilon}}_1 &= \boldsymbol{v}_1
\end{aligned}$$

$$\begin{aligned}\boldsymbol{v}_1 &= -k_{11}\left|\hat{\boldsymbol{\varepsilon}}-\boldsymbol{\varepsilon}\right|^{\alpha_2}\circ sgn(\hat{\boldsymbol{\varepsilon}}-\boldsymbol{\varepsilon})\\ &\quad -\kappa_{11}\left|\hat{\boldsymbol{\varepsilon}}-\boldsymbol{\varepsilon}\right|^{\beta_2}\circ sgn(\hat{\boldsymbol{\varepsilon}}-\boldsymbol{\varepsilon})+\boldsymbol{\varepsilon}_2\\ \dot{\boldsymbol{\varepsilon}}_2 &= -k_{12}\left|\hat{\boldsymbol{\varepsilon}}-\boldsymbol{\varepsilon}\right|^{\alpha_3}\circ sgn(\hat{\boldsymbol{\varepsilon}}-\boldsymbol{\varepsilon})\\ &\quad -\kappa_{12}\left|\hat{\boldsymbol{\varepsilon}}-\boldsymbol{\varepsilon}\right|^{\beta_3}\circ sgn(\hat{\boldsymbol{\varepsilon}}-\boldsymbol{\varepsilon})\\ \hat{\boldsymbol{d}}_1 &= \boldsymbol{\varepsilon}_1,\ \hat{\dot{\boldsymbol{d}}}_1 = \boldsymbol{\varepsilon}_2\end{aligned} \tag{14}$$

Here, $\alpha_i = i\alpha-(i-1)$, $\beta_i = i\beta-(i-1)$, $i=1,2,\ldots,l$ where $\alpha\in(1-\varepsilon,1)$ and $\beta\in(1,1+\varepsilon)$ with $0<\varepsilon<0.25$ being a sufficiently small number. The observer gains k_{1i} and κ_{1i} are assigned such that matrices

$$A_1=\begin{bmatrix}-k_{10}&1&0\\-k_{11}&0&1\\-k_{12}&0&0\end{bmatrix}$$

$$A_2=\begin{bmatrix}-\kappa_{10}&1&0\\-\kappa_{11}&0&1\\-\kappa_{12}&0&0\end{bmatrix}$$

are Hurwitz. Operator $\circ$ represents Hadamard multiplication, $\boldsymbol{\varepsilon}_1,\boldsymbol{\varepsilon}_2$ are the estimates of $\boldsymbol{d}_1,\dot{\boldsymbol{d}}_1$, respectively.

Theorem 1: Considering the observer (14), $\boldsymbol{d}_1,\dot{\boldsymbol{d}}_1$ can be estimated precisely in a fixed time

$$T_f \le \frac{\lambda_{\max}^{\rho}(P_1)}{r\mu}+\frac{1}{r_0\eta\gamma^{\eta}} \tag{15}$$

where $\mu=1-\alpha,\eta=\beta-1,r=\lambda_{\min}(Q_1)/\lambda_{\max}(P_1),r_0=\lambda_{\min}(Q_2)/\lambda_{\max}(P_2)$, the positive number $\gamma\le\lambda_{\min}(P_2)$, the symmetric positive definite matrices Q_1,Q_2,P_1,P_2 satisfy $P_1A_1+A_1^TP_1=-Q_1,P_2A_2+A_2^TP_2=-Q_2$.

Proof: Combining (14) and (13), the observer estimation error system takes the form

$$\begin{aligned}\dot{\boldsymbol{e}}_1^0 &= -k_{10}\left|\boldsymbol{e}_1^0\right|^{\alpha_1}\circ sgn(\boldsymbol{e}_1^0)-\kappa_{10}\left|\boldsymbol{e}_1^0\right|^{\beta_1}\circ sgn(\boldsymbol{e}_1^0)+\boldsymbol{e}_1^1\\ \dot{\boldsymbol{e}}_1^1 &= -k_{11}\left|\boldsymbol{e}_1^0\right|^{\alpha_2}\circ sgn(\boldsymbol{e}_1^0)-\kappa_{11}\left|\boldsymbol{e}_1^0\right|^{\beta_2}\circ sgn(\boldsymbol{e}_1^0)+\boldsymbol{e}_1^2\\ \dot{\boldsymbol{e}}_1^2 &= -k_{12}\left|\boldsymbol{e}_1^0\right|^{\alpha_3}\circ sgn(\boldsymbol{e}_1^0)-\kappa_{12}\left|\boldsymbol{e}_1^0\right|^{\beta_3}\circ sgn(\boldsymbol{e}_1^0)+\ddot{\boldsymbol{d}}_1\end{aligned} \tag{16}$$

where $\boldsymbol{e}_1^0=\boldsymbol{\varepsilon}-\hat{\boldsymbol{\varepsilon}},\boldsymbol{e}_1^1=\boldsymbol{d}_1-\boldsymbol{\varepsilon}_1,\boldsymbol{e}_1^2=\dot{\boldsymbol{d}}_1-\boldsymbol{\varepsilon}_2$. Considering the condition in Assumption 1, it follows from [16] that observer error (16) will be fixed-time convergent, and there exists a time constant T_f such that $\boldsymbol{e}_1^i(t)=0(i=0,1,2)$ for $t>T_f$.

The similar form will be adopted to estimate $\boldsymbol{d}_2$:

$$\begin{aligned}\dot{\hat{\boldsymbol{x}}}_2 &= \boldsymbol{H}(\boldsymbol{x}_1,\boldsymbol{x}_2)+\boldsymbol{G}(\boldsymbol{x}_1,\boldsymbol{x}_2)\boldsymbol{u}+\boldsymbol{v}\\ \boldsymbol{v} &= -k_{20}\left|\hat{\boldsymbol{\varepsilon}}-\boldsymbol{\varepsilon}\right|^{\alpha_1}\circ sgn(\hat{\boldsymbol{\varepsilon}}-\boldsymbol{\varepsilon})-\kappa_{20}\left|\hat{\boldsymbol{\varepsilon}}-\boldsymbol{\varepsilon}\right|^{\beta_1}\circ sgn(\hat{\boldsymbol{\varepsilon}}-\boldsymbol{\varepsilon})+\hat{\boldsymbol{d}}_2\\ \dot{\hat{\boldsymbol{d}}}_2 &= -k_{21}\left|\hat{\boldsymbol{\varepsilon}}-\boldsymbol{\varepsilon}\right|^{\alpha_2}\circ sgn(\hat{\boldsymbol{\varepsilon}}-\boldsymbol{\varepsilon})-\kappa_{21}\left|\hat{\boldsymbol{\varepsilon}}-\boldsymbol{\varepsilon}\right|^{\beta_2}\circ sgn(\hat{\boldsymbol{\varepsilon}}-\boldsymbol{\varepsilon})\end{aligned} \tag{17}$$

where all parameters are designed in the same way. Let $\boldsymbol{e}_2^0=\boldsymbol{x}_2-\hat{\boldsymbol{x}}_2,\boldsymbol{e}_2^1=\boldsymbol{d}_2-\hat{\boldsymbol{d}}_2$, where $\hat{\boldsymbol{d}}_2$ is the estimates of d_2, then the observer error system will be also fixed-time convergent, and there exists a time constant T_f such that $\boldsymbol{e}_2^i(t)=0(i=0,1,2)$ for $t>T_f$.

B. FxTDO BASED NFTSMC DESIGN

A classical nonlinear dynamic sliding variables will be designed as [6]:

$$\boldsymbol{s}=\boldsymbol{\varepsilon}+\Lambda_1 sign^{\Gamma_1}\boldsymbol{\varepsilon}+\Lambda_2 sign^{\Gamma_2}\dot{\boldsymbol{\varepsilon}}_0 \tag{18}$$

where $\dot{\boldsymbol{\varepsilon}}_0=\boldsymbol{F}(\boldsymbol{x}_1,\boldsymbol{x}_2)-\dot{\boldsymbol{x}}_d+\hat{\boldsymbol{d}}_1$, $\Lambda_1>0,\Lambda_2>0,1<\Gamma_2<\Gamma_1<2$, $sign^{\Gamma_1}\boldsymbol{\varepsilon}=|\boldsymbol{\varepsilon}|^{\Gamma_1}\circ sgn(\boldsymbol{\varepsilon})$. The derivative of $\boldsymbol{s}$ is

$$\dot{\boldsymbol{s}}=\dot{\boldsymbol{\varepsilon}}+\Lambda_1\Gamma_1|\boldsymbol{\varepsilon}|^{\Gamma_1-1}\circ\dot{\boldsymbol{\varepsilon}}+\Lambda_2\Gamma_2|\dot{\boldsymbol{\varepsilon}}_0|^{\Gamma_2-1}\circ\ddot{\boldsymbol{\varepsilon}}_0 \tag{19}$$

where

$$\begin{aligned}\ddot{\boldsymbol{\varepsilon}}_0 &= \frac{\partial\boldsymbol{F}(\boldsymbol{x}_1,\boldsymbol{x}_2)}{\partial\boldsymbol{x}_1}\dot{\boldsymbol{x}}_1+\frac{\partial\boldsymbol{F}(\boldsymbol{x}_1,\boldsymbol{x}_2)}{\partial\boldsymbol{x}_2}\dot{\boldsymbol{x}}_2-\ddot{\boldsymbol{x}}_d+\hat{\dot{\boldsymbol{d}}}_1\\ &= \frac{\partial\boldsymbol{F}(\boldsymbol{x}_1,\boldsymbol{x}_2)}{\partial\boldsymbol{x}_1}(\boldsymbol{F}(\boldsymbol{x}_1,\boldsymbol{x}_2)+\boldsymbol{d}_1)-\ddot{\boldsymbol{x}}_d+\hat{\dot{\boldsymbol{d}}}_1\\ &\quad +\frac{\partial\boldsymbol{F}(\boldsymbol{x}_1,\boldsymbol{x}_2)}{\partial\boldsymbol{x}_2}(\boldsymbol{H}(\boldsymbol{x}_1,\boldsymbol{x}_2)+\boldsymbol{G}(\boldsymbol{x}_1,\boldsymbol{x}_2)\boldsymbol{u}+\boldsymbol{d}_2)\end{aligned} \tag{20}$$

The following control law will be adopted:

$$\begin{aligned}U &= \left(\frac{\partial\boldsymbol{F}(\boldsymbol{x}_1,\boldsymbol{x}_2)}{\partial\boldsymbol{x}_2}\boldsymbol{G}(\boldsymbol{x}_1,\boldsymbol{x}_2)\right)^{\dagger}\Bigg[-\frac{\partial\boldsymbol{F}(\boldsymbol{x}_1,\boldsymbol{x}_2)}{\partial\boldsymbol{x}_2}\boldsymbol{H}(\boldsymbol{x}_1,\boldsymbol{x}_2)\\ &\quad -\frac{\partial\boldsymbol{F}(\boldsymbol{x}_1,\boldsymbol{x}_2)}{\partial\boldsymbol{x}_2}\hat{\boldsymbol{d}}_2-\frac{\partial\boldsymbol{F}(\boldsymbol{x}_1,\boldsymbol{x}_2)}{\partial\boldsymbol{x}_1}\left(\boldsymbol{F}(\boldsymbol{x}_1,\boldsymbol{x}_2)+\hat{\boldsymbol{d}}_1\right)\\ &\quad -\hat{\dot{\boldsymbol{d}}}_1+\ddot{\boldsymbol{x}}_d-\frac{1}{\Lambda_2\Gamma_2}|\dot{\boldsymbol{\varepsilon}}_0|^{2-\Gamma_2}\circ sgn\dot{\boldsymbol{\varepsilon}}_0\circ\left(\boldsymbol{I}_1+\Lambda_1\Gamma_1|\boldsymbol{\varepsilon}|^{\Gamma_1-1}\right)\\ &\quad -M_1|\boldsymbol{s}|^{\alpha}\circ sgn(\boldsymbol{s})-M_2\boldsymbol{s}\Bigg]\end{aligned} \tag{21}$$

where $0<\alpha<1,\boldsymbol{I}_1=[1,1,1]^T,M_1>0,M_2>0$. It's obvious that $\frac{\partial\boldsymbol{F}(\boldsymbol{x}_1,\boldsymbol{x}_2)}{\partial\boldsymbol{x}_2}$ is a nonsingular matrix and $\boldsymbol{G}(\boldsymbol{x}_1,\boldsymbol{x}_2)$ is a full row rank matrix, so $\boldsymbol{X}=\frac{\partial\boldsymbol{F}(\boldsymbol{x}_1,\boldsymbol{x}_2)}{\partial\boldsymbol{x}_2}\boldsymbol{G}(\boldsymbol{x}_1,\boldsymbol{x}_2)$ is a full row rank matrix and its pseudo inverse matrix can be expressed as $\boldsymbol{X}^{\dagger}=\boldsymbol{X}^T\left(\boldsymbol{X}\boldsymbol{X}^T\right)^{-1}$.

Substituting the control law (20) into (18) and (19), the following equations will be obtained:

$$\begin{aligned}\dot{\boldsymbol{s}} &= \Lambda_2\Gamma_2|\dot{\boldsymbol{\varepsilon}}_0|^{\Gamma_2-1}\circ\Bigg[\boldsymbol{e}_1^2+\frac{\partial\boldsymbol{F}(\boldsymbol{x}_1,\boldsymbol{x}_2)}{\partial\boldsymbol{x}_2}\boldsymbol{e}_2^1\\ &\quad +\frac{\partial\boldsymbol{F}(\boldsymbol{x}_1,\boldsymbol{x}_2)}{\partial\boldsymbol{x}_1}\boldsymbol{e}_1^1-M_1|\boldsymbol{s}|^{\alpha}\circ sgn(\boldsymbol{s})-M_2\boldsymbol{s}\Bigg]\\ &\quad +\left(\boldsymbol{I}_1+\Lambda_1\Gamma_1|\varepsilon|^{\Gamma_1-1}\right)\circ\boldsymbol{e}_1^1\end{aligned} \tag{22}$$

$$\begin{aligned}\ddot{\boldsymbol{\varepsilon}}_0 &= \boldsymbol{e}_1^2+\frac{\partial\boldsymbol{F}(\boldsymbol{x}_1,\boldsymbol{x}_2)}{\partial\boldsymbol{x}_2}\boldsymbol{e}_2^1+\frac{\partial\boldsymbol{F}(\boldsymbol{x}_1,\boldsymbol{x}_2)}{\partial\boldsymbol{x}_1}\boldsymbol{e}_1^1\\ &\quad -M_1|\boldsymbol{s}|^{\alpha}\circ sgn(\boldsymbol{s})-M_2\boldsymbol{s}\\ &\quad -\frac{1}{\Lambda_2\Gamma_2}|\dot{\boldsymbol{\varepsilon}}_0|^{2-\Gamma_2}\circ sgn\dot{\boldsymbol{\varepsilon}}_0\circ\left(\boldsymbol{I}_1+\Lambda_1\Gamma_1|\boldsymbol{\varepsilon}|^{\Gamma_1-1}\right)\end{aligned} \tag{23}$$

Theorem 2: Considering system (13) with mismatched disturbance, the control law (21) with FxTDO is adopted, then Lyapunov function $V_1=(1/2)\left(\boldsymbol{s}^T\boldsymbol{s}+\boldsymbol{\varepsilon}^T\boldsymbol{\varepsilon}+\dot{\boldsymbol{\varepsilon}}_0^T\dot{\boldsymbol{\varepsilon}}_0\right)$ will be finite-time bounded.

Proof: the proof will be given in Appendix.

Since V_1 is finite-time bounded, then $\boldsymbol{s},\boldsymbol{\varepsilon},\dot{\boldsymbol{\varepsilon}}_0$ won't escape to infinity before observer errors converge to zero. Once the

observer errors reach zero, (22) will be transformed into the following formulation

$$\dot{\boldsymbol{s}} = \Lambda_2\Gamma_2 \left|\dot{\boldsymbol{e}}_0\right|^{\Gamma_2-1} \circ \left[-M_1 \left|\boldsymbol{s}\right|^{\alpha} \circ sgn(\boldsymbol{s}) - M_2\boldsymbol{s}\right] \quad (24)$$

Define another Lyapunov function $V_2 = 0.5\boldsymbol{s}^T\boldsymbol{s}$, then

$$\begin{aligned}\dot{V}_2 &= \boldsymbol{s}^T\left(\Lambda_2\Gamma_2 \left|\dot{\boldsymbol{e}}_0\right|^{\Gamma_2-1} \circ \left[-M_1 \left|\boldsymbol{s}\right|^{\alpha} \circ sgn(\boldsymbol{s}) - M_2\boldsymbol{s}\right]\right)\\ &\le -\rho_1\left(\dot{\boldsymbol{e}}_0\right) V_2^{(1+\alpha)/2} - \rho_2\left(\dot{\boldsymbol{e}}_0\right) V_2 \end{aligned} \quad (25)$$

where

$$\begin{aligned}\rho_1\left(\dot{\boldsymbol{e}}_0\right) &= 2^{(1+\alpha)/2}\Lambda_2\Gamma_2 M_1 \min_i \left|\dot{\boldsymbol{e}}_{0i}\right|^{\Gamma_2-1},\\ \rho_2\left(\dot{\boldsymbol{e}}_0\right) &= 2\Lambda_2\Gamma_2 M_2 \min_i \left|\dot{\boldsymbol{e}}_{0i}\right|^{\Gamma_2-1}.\end{aligned}$$

When $\dot{\boldsymbol{e}}_0 = 0$, Equ. (22) becomes:

$$\ddot{\boldsymbol{e}}_0 = -M_1 \left|\boldsymbol{s}\right|^{\alpha} \circ sgn(\boldsymbol{s}) - M_2\boldsymbol{s} \quad (26)$$

It's evident that $\dot{\boldsymbol{e}}_0 = 0$ isn't an attractor, so the system will keep moving until reaching the sliding mode surface. Therefore, it can be concluded that system (24) is finite- time stable.

After reaching the sliding mode surface, the partial dynamic system will be $\boldsymbol{\varepsilon} + \Lambda_1 sign^{\Gamma_1}\boldsymbol{\varepsilon} + \Lambda_2 sign^{\Gamma_2}\dot{\boldsymbol{\varepsilon}} = 0$, which will converge to the origin with fast convergence.

However, FxTDO based terminal sliding mode control method cannot guarantee the output tracking error constraints before the disturbance observer tracking errors converge to a small prescribed range. Consequently, barrier Lyapunov function based terminal sliding mode control will be adopted.

C. BARRIER LYAPUNOV BASED NFTSMC DESIGN

Considering the output tracking error constraints, our main approach is to constrain the sliding mode variables, the following barrier Lyapunov function is adopted

$$V = \frac{1}{2}\sum_{i=1}^{3}\log\left(\frac{k_i^2}{k_i^2 - s_i^2}\right) \quad (27)$$

where $k_i = c_{i1}e^{-c_{i2}|\varepsilon_i|} + c_{i3}(i = 1, 2, 3)$ with c_{i1}, c_{i2} and c_{i3} being nonnegative constants, $\boldsymbol{s} = [s_1, s_2, s_3]$. The sliding variables adopt the same form of (17).

The derivative of V is given

$$\begin{aligned}\dot{V} &= \frac{1}{2}\sum_{i=1}^{3}\frac{k_i^2 - s_i^2}{k_i^2}\frac{2k_i\dot{k}_i\left(k_i^2 - s_i^2\right) - k_i^2\left(2k_i\dot{k}_i - 2s_i\dot{s}_i\right)}{\left(k_i^2 - s_i^2\right)^2}\\ &= \sum_{i=1}^{3}\frac{s_i\left(\dot{s}_i - \left(\dot{k}_i/k_i\right)s_i\right)}{\left(k_i^2 - s_i^2\right)}\\ &= \boldsymbol{J}\left(\dot{\boldsymbol{s}} - \boldsymbol{K}\boldsymbol{s}\right)\end{aligned} \quad (28)$$

where $\boldsymbol{J} = \left[\frac{s_1}{k_1^2-s_1^2}, \frac{s_2}{k_2^2-s_2^2}, \frac{s_3}{k_3^2-s_3^2}\right]$, $\boldsymbol{K} = diag\left(\frac{\dot{k}_1}{k_1}, \frac{\dot{k}_2}{k_2}, \frac{\dot{k}_3}{k_3}\right)$.

To simplify the control design and guarantee finite-time convergence, the control laws are divided into two categories. The first category will guarantee the sliding variables constraints before disturbance observer tracking errors converge to a small prescribed range, the second category will guarantee the finite-time convergence of output tracking errors with sliding variables constraints.

1) While $|s_i| > \left|k_i - c_{i1}/2\right|$ $(i = 1, 2, 3)$ and $t \le T_f$, then the following control law will be adopted:

$$\begin{aligned}\boldsymbol{u} = &\left(\frac{\partial \boldsymbol{F}(\boldsymbol{x}_1, \boldsymbol{x}_2)}{\partial \boldsymbol{x}_2}\boldsymbol{G}(\boldsymbol{x}_1, \boldsymbol{x}_2)\right)^{\dagger}\left[-\frac{\partial \boldsymbol{F}(\boldsymbol{x}_1, \boldsymbol{x}_2)}{\partial \boldsymbol{x}_2}\boldsymbol{H}(\boldsymbol{x}_1, \boldsymbol{x}_2)\right.\\ &-\frac{\partial \boldsymbol{F}(\boldsymbol{x}_1, \boldsymbol{x}_2)}{\partial \boldsymbol{x}_2}\hat{\boldsymbol{d}}_2 - \frac{\partial \boldsymbol{F}(\boldsymbol{x}_1, \boldsymbol{x}_2)}{\partial \boldsymbol{x}_1}\left(\boldsymbol{F}(\boldsymbol{x}_1, \boldsymbol{x}_2) + \hat{\boldsymbol{d}}_1\right)\\ &-\dot{\hat{\boldsymbol{d}}}_1 + \ddot{\boldsymbol{x}}_d - \frac{1}{\Lambda_2\Gamma_2}\left|\dot{\boldsymbol{e}}_0\right|^{2-\Gamma_2} \circ sgn\dot{\boldsymbol{e}}_0 \circ \left(\boldsymbol{I}_1 + \Lambda_1\Gamma_1\left|\boldsymbol{\varepsilon}\right|^{\Gamma_1-1}\right)\\ &\left.-M_1\boldsymbol{K}_{\alpha}\left|\boldsymbol{s}\right|^{\alpha} \circ sgn(\boldsymbol{s}) - M_2\boldsymbol{K}_{\gamma}\boldsymbol{s} - \frac{1}{\Lambda_2\Gamma_2}\left|\dot{\boldsymbol{e}}_0\right|^{2-\Gamma_2} \circ \boldsymbol{K}_{\beta}\boldsymbol{s}\right]\end{aligned} \quad (29)$$

where $\boldsymbol{K}_{\alpha} = diag\left((k_1 - s_1)^{\frac{1-\alpha}{2}}, (k_2 - s_2)^{\frac{1-\alpha}{2}}, (k_3 - s_3)^{\frac{1-\alpha}{2}}\right)$, $\boldsymbol{K}_{\beta} = diag\left(c_{12}, c_{22}, c_{32}\right)$, $\boldsymbol{K}_{\gamma} = diag\left(\frac{1}{k_1^2-s_1^2}, \frac{1}{k_2^2-s_2^2}, \frac{1}{k_3^2-s_3^2}\right)$.

Then substituting the control law (29) into Equ. (19):

$$\begin{aligned}\dot{\boldsymbol{s}} = &\Lambda_2\Gamma_2\left|\dot{\boldsymbol{e}}_0\right|^{\Gamma_2-1} \circ \left[\boldsymbol{e}_1^2 + \frac{\partial \boldsymbol{F}(\boldsymbol{x}_1, \boldsymbol{x}_2)}{\partial \boldsymbol{x}_2}\boldsymbol{e}_2^1 + \frac{\partial \boldsymbol{F}(\boldsymbol{x}_1, \boldsymbol{x}_2)}{\partial \boldsymbol{x}_1}\boldsymbol{e}_1^1\right.\\ &\left.-M_1\boldsymbol{K}_{\alpha}\left|\boldsymbol{s}\right|^{\alpha} \circ sgn(\boldsymbol{s}) - M_2\boldsymbol{K}_{\gamma}\boldsymbol{s}\right] - \left|\dot{\boldsymbol{e}}_0\right| \circ \boldsymbol{K}_{\beta}\boldsymbol{s}\\ &+\left(\boldsymbol{I}_1 + \Lambda_1\Gamma_1\left|\varepsilon\right|^{\Gamma_1-1}\right) \circ \boldsymbol{e}_1^1\end{aligned} \quad (30)$$

When s_i approaches k_i, $\boldsymbol{K}_{\gamma i}$ becomes infinity, then $|s_i|$ will decrease sharply, so never will s_i exceed k_i in this case.

2) While $|s_i| \le \left|k_i - c_{i1}/2\right|$ $(i = 1, 2, 3)$ or $t > T_f$, then the following control law will be adopted:

$$\begin{aligned}\boldsymbol{u} = &\left(\frac{\partial \boldsymbol{F}(\boldsymbol{x}_1, \boldsymbol{x}_2)}{\partial \boldsymbol{x}_2}\boldsymbol{G}(\boldsymbol{x}_1, \boldsymbol{x}_2)\right)^{\dagger}\left[-\frac{\partial \boldsymbol{F}(\boldsymbol{x}_1, \boldsymbol{x}_2)}{\partial \boldsymbol{x}_2}\boldsymbol{H}(\boldsymbol{x}_1, \boldsymbol{x}_2)\right.\\ &-\frac{\partial \boldsymbol{F}(\boldsymbol{x}_1, \boldsymbol{x}_2)}{\partial \boldsymbol{x}_2}\hat{\boldsymbol{d}}_2 - \frac{\partial \boldsymbol{F}(\boldsymbol{x}_1, \boldsymbol{x}_2)}{\partial \boldsymbol{x}_1}\left(\boldsymbol{F}(\boldsymbol{x}_1, \boldsymbol{x}_2) + \hat{\boldsymbol{d}}_1\right)\\ &-\dot{\hat{\boldsymbol{d}}}2_1 + \ddot{\boldsymbol{x}}_d - \frac{1}{\Lambda_2\Gamma_2}\left|\dot{\boldsymbol{e}}_0\right|^{2-\Gamma_2} \circ sgn\dot{\boldsymbol{e}}_0 \circ \left(\boldsymbol{I}_1 + \Lambda_1\Gamma_1\left|\boldsymbol{\varepsilon}\right|^{\Gamma_1-1}\right)\\ &\left.-M_1\boldsymbol{K}_{\alpha}\left|\boldsymbol{s}\right|^{\alpha} \circ sgn(\boldsymbol{s}) - M_2\boldsymbol{s} - \frac{1}{\Lambda_2\Gamma_2}\left|\dot{\boldsymbol{e}}_0\right|^{2-\Gamma_2} \circ \boldsymbol{K}_{\beta}\boldsymbol{s}\right]\end{aligned} \quad (31)$$

where $\boldsymbol{K}_{\alpha}, \boldsymbol{K}_{\beta}$ have the same forms of (29).

Then substituting the control law (31) into the derivative of sliding variables $\boldsymbol{s}$ (19):

$$\begin{aligned}\dot{\boldsymbol{s}} = &\Lambda_2\Gamma_2\left|\dot{\boldsymbol{e}}_0\right|^{\Gamma_2-1} \circ \left[\boldsymbol{e}_1^2 + \frac{\partial \boldsymbol{F}(\boldsymbol{x}_1, \boldsymbol{x}_2)}{\partial \boldsymbol{x}_2}\boldsymbol{e}_2^1 + \frac{\partial \boldsymbol{F}(\boldsymbol{x}_1, \boldsymbol{x}_2)}{\partial \boldsymbol{x}_1}\boldsymbol{e}_1^1\right.\\ &\left.-M_1\boldsymbol{K}_{\alpha}\left|\boldsymbol{s}\right|^{\alpha} \circ sgn(\boldsymbol{s}) - M_2\boldsymbol{s}\right] - \left|\dot{\boldsymbol{e}}_0\right| \circ \boldsymbol{K}_{\beta}\boldsymbol{s}\\ &+\left(\boldsymbol{I}_1 + \Lambda_1\Gamma_1\left|\varepsilon\right|^{\Gamma_1-1}\right) \circ \boldsymbol{e}_1^1\end{aligned} \quad (32)$$

Substituting (32) into (28) results in

$$\begin{aligned}\dot{V} &= \boldsymbol{J}(\dot{\boldsymbol{s}} - \boldsymbol{K}\boldsymbol{s}) \\ &= \boldsymbol{J}\left(\Lambda_2\Gamma_2 \left|\dot{\boldsymbol{e}}_0\right|^{\Gamma_2-1} \circ \left[\boldsymbol{e}_1^2 + \frac{\partial \boldsymbol{F}(\boldsymbol{x}_1, \boldsymbol{x}_2)}{\partial \boldsymbol{x}_2}\boldsymbol{e}_2^1 + \frac{\partial \boldsymbol{F}(\boldsymbol{x}_1, \boldsymbol{x}_2)}{\partial \boldsymbol{x}_1}\boldsymbol{e}_1^1\right]\right) \\ &\quad - \boldsymbol{J}\left(\Lambda_2\Gamma_2 \left|\dot{\boldsymbol{e}}_0\right|^{\Gamma_2-1} \circ \left[M_1\boldsymbol{K}_\alpha |\boldsymbol{s}|^\alpha \circ sgn(\boldsymbol{s}) + M_2\boldsymbol{s}\right]\right) \\ &\quad - \boldsymbol{J}\left|\dot{\boldsymbol{e}}_0\right| \circ \boldsymbol{K}_\beta\boldsymbol{s} + \boldsymbol{J}\left(\left(\boldsymbol{I}_1 + \Lambda_1\Gamma_1 |\varepsilon|^{\Gamma_1-1}\right) \circ \boldsymbol{e}_1^1 - \boldsymbol{K}\boldsymbol{s}\right)\end{aligned} \tag{33}$$

Obviously the first category control law will guarantee the sliding variables constraints while $t \leq T_f$, then $\boldsymbol{\varepsilon}$ and $\dot{\boldsymbol{e}}_0$ won't escape to infinity according to the following Theorem 3. Once the observer errors reach zero, then

$$\begin{aligned}\dot{V} &= \boldsymbol{J}(\dot{\boldsymbol{s}} - \boldsymbol{K}\boldsymbol{s}) \\ &= -\boldsymbol{J}\left(\Lambda_2\Gamma_2 \left|\dot{\boldsymbol{e}}_0\right|^{\Gamma_2-1} \circ \left[M_1\boldsymbol{K}_\alpha |\boldsymbol{s}|^\alpha \circ sgn(\boldsymbol{s}) + M_2\boldsymbol{s}\right]\right) \\ &\quad - \boldsymbol{J}\left|\dot{\boldsymbol{e}}_0\right| \circ \boldsymbol{K}_\beta\boldsymbol{s} - \boldsymbol{J}\boldsymbol{K}\boldsymbol{s}\end{aligned} \tag{34}$$

Besides, the following inequalities can be set

$$\boldsymbol{K} \geq diag\left(-c_{12}\left|\dot{\varepsilon}_1\right|, -c_{22}\left|\dot{\varepsilon}_2\right|, -c_{32}\left|\dot{\varepsilon}_3\right|\right) \tag{35}$$

$$\left\|\|\dot{\boldsymbol{e}}\| - \|\dot{\boldsymbol{e}}_0\|\right\| \leq \left\|\left\|\dot{\boldsymbol{e}}_0 + \boldsymbol{e}_1^1\right\| - \|\dot{\boldsymbol{e}}_0\|\right\| \leq \left\|\boldsymbol{e}_1^1\right\| \tag{36}$$

Then

$$\dot{V} \leq -\boldsymbol{J}\left(\Lambda_2\Gamma_2 \left|\dot{\boldsymbol{e}}_0\right|^{\Gamma_2-1} \circ \left[M_1\boldsymbol{K}_\alpha |\boldsymbol{s}|^\alpha \circ sgn(\boldsymbol{s}) + M_2\boldsymbol{s}\right]\right) \tag{37}$$

Since $\log(x) \leq x - 1$ for $x \geq 1$, then

$$\dot{V} \leq -\Lambda_2\Gamma_2\left(\min_i \left|\dot{\boldsymbol{e}}_{0i}\right|^{\Gamma_2-1}\right)\left(M_1 V^{(\alpha+1)/2} + M_2 V\right) \tag{38}$$

In the same way, $\dot{\boldsymbol{e}}_0 = 0$ isn't an attractor, so the system will keep moving until reaching the sliding mode surface. Therefore, it can be concluded that system (38) is finite- time stable.

Before disturbance observer tracking errors converge to a small prescribed range, it's hard to predict the trajectory of sliding variables, so it's meaningful to constrain sliding variables in the initial period in order to constrain the outputs tracking errors.

Theorem 3: When the sliding variables satisfy the constraints $\left|\varepsilon_i + \Lambda_1 sign^{\Gamma_1}\varepsilon_i + \Lambda_2 sign^{\Gamma_2}\dot{\varepsilon}_{0i}\right| \leq c_{i1}e^{-c_{i2}|\varepsilon_i|} + c_{i3}$, for $i = 1, 2, 3$, then outputs will never exceed the region $[\min\{\varepsilon_{ic}, \varepsilon_{id}\}, \max\{\varepsilon_{ia}, \varepsilon_{ib}\}]$.

Proof: The proof is divided into four parts:

1) if $\varepsilon_i > 0$ and $e_{1i}^1 > 0$, then:

$$\varepsilon_i + \Lambda_1 sign^{\Gamma_1}\varepsilon_i + \Lambda_2 sign^{\Gamma_2}\left(\dot{\varepsilon}_i - e_{1i}^1\right) \leq c_{i1}e^{-c_{i2}|\varepsilon_i|} + c_{i3} \tag{39}$$

Let ε_{ia} satisfies $\varepsilon_{ia} + \Lambda_1\varepsilon_{ia}^{\Gamma_1} = c_{i1}e^{-c_{i2}|\varepsilon_{ia}|} + c_{i3} + \Lambda_2 e_{1i}^{1\,\Gamma_2}$. Define $f(\varepsilon_{ia}) = \varepsilon_{ia} + \Lambda_1\varepsilon_{ia}^{\Gamma_1}$ and $g(\varepsilon_{ia}) = c_{i1}e^{-c_{i2}|\varepsilon_{ia}|} + c_{i3} + \Lambda_2 e_{1i}^{1\,\Gamma_2}$, since $f(\varepsilon_{ia})$ is monotonous increasing function and $g(\varepsilon_{ia})$ is monotonous decreasing function while $\varepsilon_{ia} > 0$, besides $f(\varepsilon_{ia})$ is odd and coercive function, so equation $f(\varepsilon_{ia}) = g(\varepsilon_{ia})$ has a unique solution. If $\varepsilon_i > \varepsilon_{ia}$, then $\dot{\varepsilon}_i < 0$, so the ε_i will decrease. Considering the continuity and initial condition of ε_i, ε_i will never exceed the ε_{ia}.

2) if $\varepsilon_i > 0$ and $e_{1i}^1 < 0$, then:

$$\varepsilon_i + \Lambda_1 sign^{\Gamma_1}\varepsilon_i + \Lambda_2 sign^{\Gamma_2}\left(\dot{\varepsilon}_i - e_{1i}^1\right) \leq c_{i1}e^{-c_{i2}|\varepsilon_i|} + c_{i3} \tag{40}$$

Let ε_{ib} satisfies $\varepsilon_{ib} + \Lambda_1\varepsilon_{ib}^{\Gamma_1} = c_{i1}e^{-c_{i2}|\varepsilon_{ib}|} + c_{i3} + \Lambda_2 e_{1i}^{1\,\Gamma_2}$. Similarly, the existence of ε_{ib} can be verified. If $\varepsilon_i > \varepsilon_{ib}$, then $\dot{\varepsilon}_i < 0$, so the ε_i will decrease. Considering the continuity and initial condition of ε_i, ε_i will never exceed the ε_{ib}.

3) if $\varepsilon_i < 0$ and $e_{1i}^1 > 0$, then:

$$\varepsilon_i + \Lambda_1 sign^{\Gamma_1}\varepsilon_i + \Lambda_2 sign^{\Gamma_2}\left(\dot{\varepsilon}_i - e_{1i}^1\right) \geq -c_{i1}e^{-c_{i2}|\varepsilon_i|} - c_{i3} \tag{41}$$

Let ε_{ic} satisfies $\varepsilon_{ic} + \Lambda_1\varepsilon_{ic}^{\Gamma_1} = -c_{i1}e^{-c_{i2}|\varepsilon_{ic}|} - c_{i3} + \Lambda_2 e_{1i}^{1\,\Gamma_2}$. Similarly, the existence of ε_{ic} can be verified. If $\varepsilon_i < \varepsilon_{ic}$, then $\dot{\varepsilon}_i > 0$, so the ε_i will increase. Considering the continuity and initial condition of ε_i, ε_i will never exceed the ε_{ic}.

4) if $\varepsilon_i < 0$ and $e_{1i}^1 < 0$, then:

$$\varepsilon_i + \Lambda_1 sign^{\Gamma_1}\varepsilon_i + \Lambda_2 sign^{\Gamma_2}\left(\dot{\varepsilon}_i - e_{1i}^1\right) \geq -c_{i1}e^{-c_{i2}|\varepsilon_i|} - c_{i3} \tag{42}$$

Let ε_{id} satisfies $\varepsilon_{id} + \Lambda_1\varepsilon_{id}^{\Gamma_1} = -c_{i1}e^{-c_{i2}|\varepsilon_{id}|} - c_{i3} + \Lambda_2 e_{1i}^{1\,\Gamma_2}$. Similarly, the existence of ε_{id} can be verified. If $\varepsilon_i < \varepsilon_{id}$, then $\dot{\varepsilon}_i > 0$, so the ε_i will increase. Considering the continuity and initial condition of ε_i, ε_i will never exceed the ε_{id}.

In conclusion, the ε_i will never exceed the region $[\min\{\varepsilon_{ic}, \varepsilon_{id}\}, \max\{\varepsilon_{ia}, \varepsilon_{ib}\}]$. Besides, the parameters of this region can be solved by some numerical analysis methods such as Newton method and dichotomy.

V. SIMULATION RESULTS

In order to illustrate the effectiveness of the FxTDO based NFTSMC and BLF based NFTSMC design for the blended-wing-body aircraft attitude tracking, two simulation cases and comparison results will be presented in this section.

The BWB aircraft relevant parameters are chosen as

$$J = \begin{bmatrix} 1.017 & 0 & 0 \\ 0 & 0.738 & 0 \\ 0 & 0 & 1.692 \end{bmatrix}.$$

Its aerodynamic forces and torques coefficients will be given in the forms of charts. The initial states value are given by $(\alpha_0, \beta_0, \mu_0) = (0, 0, 0)$, $(p_0, q_0, r_0) = (0, 0, 0)$, and the commanded attitude angle is set as

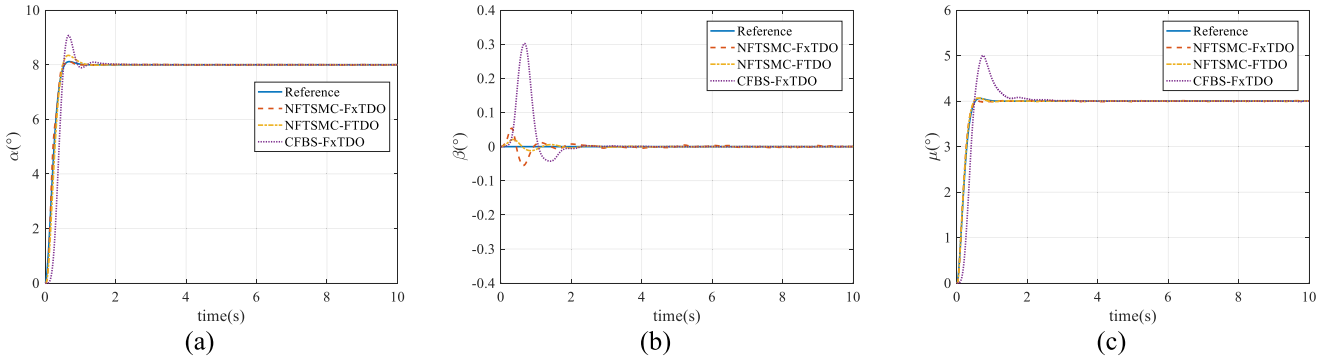

FIGURE 3. BWB aircraft attitude tracking response.

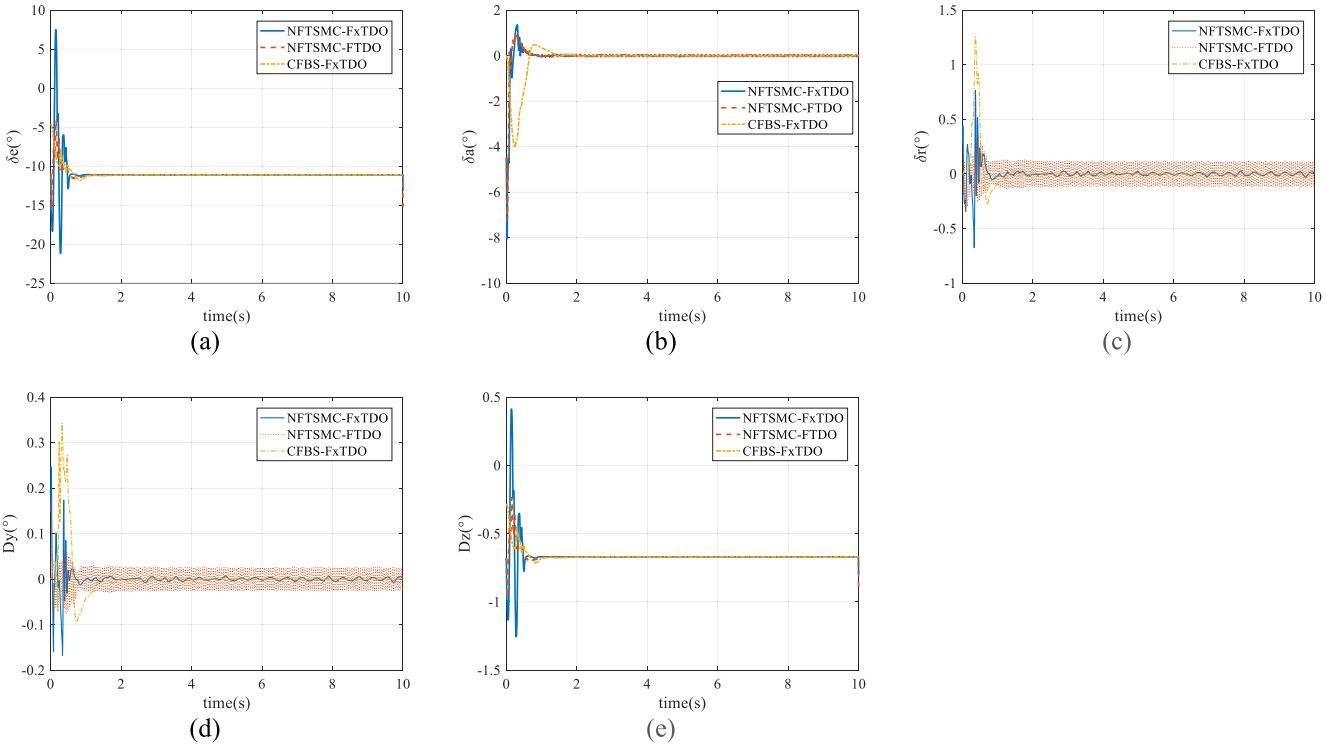

FIGURE 4. BWB aircraft actuators.

$(\alpha_c, \beta_c, \mu_c) = (8°, 0°, 4°)$, then it will pass the command filter $64/(s^2 + 12.8s + 64)$. In this paper, the disturbances are mainly resulted from dynamic model errors.

A. CASE I

In this case, the FxTDO based NFTSMC are designed for BWB aircraft attitude tracking with mismatched disturbances, moreover finite-time disturbance observer (FTDO) based NFTSMC and FxTDO based command filtered back-stepping (CFBS) are designed for comparison. The FxTDO and NFTSMC parameters are selected according to simulation tuning to achieve the prescribed performance, which are shown in the Table 1:

Besides, in the simulation the sign function is substituted by the saturation function for chattering attenuation. The attitude tracking process and control inputs are shown in Fig. 3 and Fig. 4, the FxTDO based NFTSMC and FTDO based NFTSMC's tracking performances such as overshoot, response time and tracking accuracy are better than FxTDO based CFBS's, since NFTSMC method has strong robustness and quick response. Moreover, the FxTDO based NFTSMC's actuators inputs are smoother than FTDO based NFTSMC's, the latter method's actuators chattering problem is severe. This simulation adopts non-recursive FxTDO and recursive FTDO, since non-recursive form doesn't need the sign function of the high order derivative, which makes it smoother..

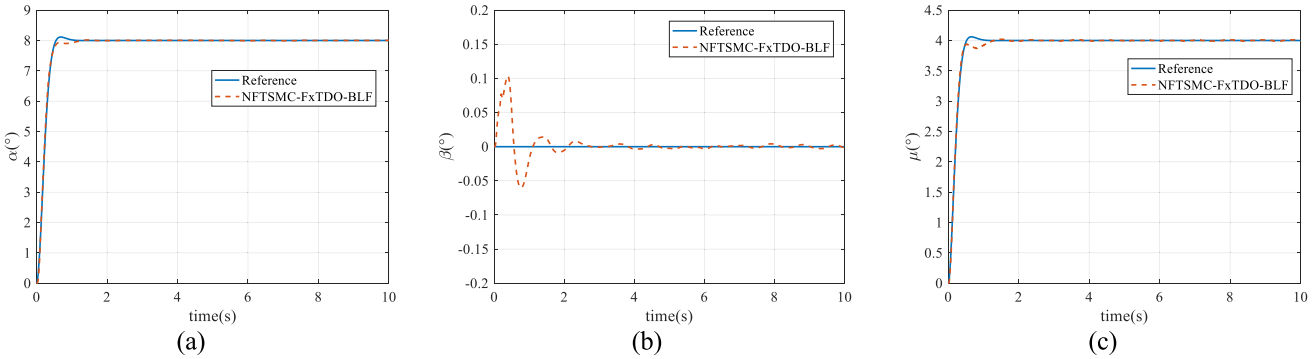

FIGURE 5. BWB aircraft attitude tracking response.

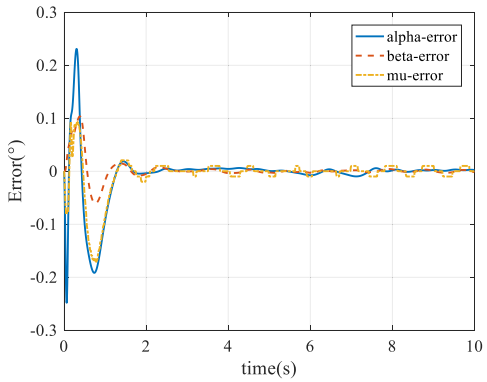

FIGURE 6. BWB aircraft attitude tracking errors.

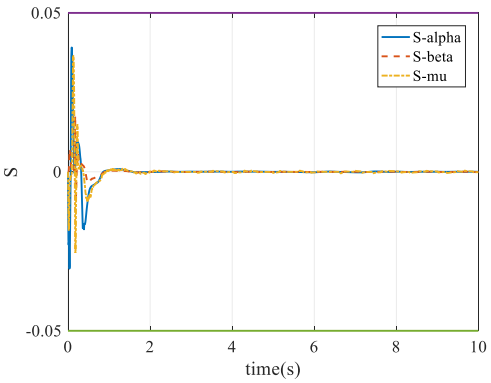

FIGURE 7. Sliding mode surfaces.

In conclusion, the FxTDO based NFTSMC performs better than others.

B. CASE II

In this case, barrier Lyapunov function (BLF) based NFTSMC is designed for BWB aircraft attitude tracking with mismatched disturbances and output constraints. The output tracking errors constraints will be bounded by $[-0.5°, 0.5°]$. The parameters for FxTDO and NFTSMC are chosen to be the same as those in case I, the parameters of sliding variable constraints are chosen as $(c_{11}, c_{21}, c_{31}) = (0.05, 0.05, 0.05)$, $(c_{12}, c_{22}, c_{32}) = (0, 0, 0)$, $(c_{13}, c_{23}, c_{33}) = (0, 0, 0)$ in this case for convenience. The attitude tracking process and tracking errors are shown in Fig. 5 and Fig. 6, which indicates that attitude tracking errors satisfy the output constraints. In Fig. 7, the sliding variables are constrained in the given region.

TABLE 1. Control scheme parameters.

Control Terms	Parameter Values [a]
Outer Loop FxTDO	$k_{10} = 800$, $\kappa_{10} = 800$, $k_{11} = 200$, $\kappa_{11} = 200$, $k_{12} = 200$, $\kappa_{12} = 200$, $\alpha = 0.9$, $\beta = 1.1$
Inter Loop FxTDO	$k_{20} = 200$, $\kappa_{20} = 200$, $k_{21} = 600$, $\kappa_{21} = 600$, $\alpha = 0.8$, $\beta = 1.2$
NFTSMC	$\Lambda_1 = \Lambda_2 = 2$, $\Gamma_1 = 5/3$, $\Gamma_2 = 7/5$, $M_1 = 40$, $M_2 = 30$

VI. CONCLUSION

This paper presents a barrier Lyapunov function based non-singular fast terminal sliding mode control with fixed-time non-recursive disturbance observer for the blended-wing-body (BWB) aircraft high-precision attitude tracking in the presence of mismatched disturbances and output constraints. The fixed-time non-recursive disturbance observer can attenuate matched and mismatched disturbance, and the barrier Lyapunov function can be developed to constrain the sliding variables to achieve high-precision attitude tracking. The effectiveness of the proposed control scheme have been verified in the numerical simulation. In the future, how to constrain the sliding mode surfaces in the presence of disturbances will be another meaningful idea.

APPENDIX

The Lyapunov function is chosen as:

$$v_1 = \frac{1}{2}\boldsymbol{s}^T\boldsymbol{s} + \frac{1}{2}\boldsymbol{\varepsilon}^T\boldsymbol{\varepsilon} + \frac{1}{2}\dot{\boldsymbol{\varepsilon}}_0^T\dot{\boldsymbol{\varepsilon}}_0 \tag{43}$$

The derivative of Lyapunov function is:

$$\begin{aligned}\dot{V}_1 &= \boldsymbol{s}^T\dot{\boldsymbol{s}} + \boldsymbol{\varepsilon}^T\dot{\boldsymbol{\varepsilon}} + \dot{\boldsymbol{e}}_0^T\ddot{\boldsymbol{e}}_0 \\ &= \boldsymbol{s}^T\Bigg[\Lambda_2\Gamma_2\left|\dot{\boldsymbol{e}}_0\right|^{\Gamma_2-1}\circ\Bigg[\boldsymbol{e}_1^2 + \frac{\partial \boldsymbol{F}(\boldsymbol{x}_1,\boldsymbol{x}_2)}{\partial \boldsymbol{x}_2}\boldsymbol{e}_2^1 \\ &\quad + \frac{\partial \boldsymbol{F}(\boldsymbol{x}_1,\boldsymbol{x}_2)}{\partial \boldsymbol{x}_1}\boldsymbol{e}_1^1 - M_1\left|\boldsymbol{s}\right|^{\alpha}\circ sgn(\boldsymbol{s}) - M_2\boldsymbol{s}\Bigg] \\ &\quad + \left(\boldsymbol{I}_1 + \Lambda_1\Gamma_1\left|\varepsilon\right|^{\Gamma_1-1}\right)\circ\boldsymbol{e}_1^1\Bigg] + \boldsymbol{\varepsilon}^T\left[\boldsymbol{F}(\boldsymbol{x}_1,\boldsymbol{x}_2)\right. \\ &\quad \left. - \dot{\boldsymbol{x}}_d + \boldsymbol{d}_1\right] + \dot{\boldsymbol{e}}_0^T\Bigg[\boldsymbol{e}_1^2 + \frac{\partial \boldsymbol{F}(\boldsymbol{x}_1,\boldsymbol{x}_2)}{\partial \boldsymbol{x}_2}\boldsymbol{e}_2^1 + \frac{\partial \boldsymbol{F}(\boldsymbol{x}_1,\boldsymbol{x}_2)}{\partial \boldsymbol{x}_1}\boldsymbol{e}_1^1 \\ &\quad - M_1\left|\boldsymbol{s}\right|^{\alpha}\circ sgn(\boldsymbol{s}) - M_2\boldsymbol{s} \\ &\quad - \frac{1}{\Lambda_2\Gamma_2}\left|\dot{\boldsymbol{e}}_0\right|^{2-\Gamma_2}\circ sgn\dot{\boldsymbol{e}}_0\circ\left(\boldsymbol{I}_1 + \Lambda_1\Gamma_1\left|\boldsymbol{\varepsilon}\right|^{\Gamma_1-1}\right)\Bigg]\end{aligned} \tag{44}$$

It's easy to verify the following inequalities:

$$\begin{aligned}&\boldsymbol{s}^T\left[\Lambda_2\Gamma_2\left|\dot{\boldsymbol{e}}_0\right|^{\Gamma_2-1}\circ M_1\left|\boldsymbol{s}\right|^{\alpha}\circ sgn(\boldsymbol{s})\right] \geq 0 \\ &\boldsymbol{s}^T\left[\Lambda_2\Gamma_2\left|\dot{\boldsymbol{e}}_0\right|^{\Gamma_2-1}\circ M_2\boldsymbol{s}\right] \geq 0 \\ &\dot{\boldsymbol{e}}_0^T\left[\frac{1}{\Lambda_2\Gamma_2}\left|\dot{\boldsymbol{e}}_0\right|^{2-\Gamma_2}\circ sgn\dot{\boldsymbol{e}}_0\circ\left(\boldsymbol{I}_1 + \Lambda_1\Gamma_1\left|\boldsymbol{\varepsilon}\right|^{\Gamma_1-1}\right)\right] \geq 0\end{aligned} \tag{45}$$

Then Equ. (44) can be transformed as below:

$$\begin{aligned}\dot{V}_1 &= \boldsymbol{s}^T\dot{\boldsymbol{s}} + \boldsymbol{\varepsilon}^T\dot{\boldsymbol{\varepsilon}} + \dot{\boldsymbol{e}}_0^T\ddot{\boldsymbol{e}}_0 \\ &\leq \boldsymbol{s}^T\Bigg[\Lambda_2\Gamma_2\left|\dot{\boldsymbol{e}}_0\right|^{\Gamma_2-1}\circ\Bigg[\boldsymbol{e}_1^2 + \frac{\partial \boldsymbol{F}(\boldsymbol{x}_1,\boldsymbol{x}_2)}{\partial \boldsymbol{x}_2}\boldsymbol{e}_2^1 \\ &\quad + \frac{\partial \boldsymbol{F}(\boldsymbol{x}_1,\boldsymbol{x}_2)}{\partial \boldsymbol{x}_1}\boldsymbol{e}_1^1\Bigg] + \left(\boldsymbol{I}_1 + \Lambda_1\Gamma_1\left|\varepsilon\right|^{\Gamma_1-1}\right)\circ\boldsymbol{e}_1^1\Bigg] \\ &\quad + \boldsymbol{\varepsilon}^T\left[\dot{\boldsymbol{e}}_0 + \boldsymbol{e}_1^1\right] + \dot{\boldsymbol{e}}_0^T\Bigg[\boldsymbol{e}_1^2 + \frac{\partial \boldsymbol{F}(\boldsymbol{x}_1,\boldsymbol{x}_2)}{\partial \boldsymbol{x}_2}\boldsymbol{e}_2^1 \\ &\quad + \frac{\partial \boldsymbol{F}(\boldsymbol{x}_1,\boldsymbol{x}_2)}{\partial \boldsymbol{x}_1}\boldsymbol{e}_1^1 - M_1\left|\boldsymbol{s}\right|^{\alpha}\circ sgn(\boldsymbol{s}) - M_2\boldsymbol{s}\Bigg]\end{aligned} \tag{46}$$

It's convenient to prove that $\|\boldsymbol{x}\circ\boldsymbol{y}\| \leq \|\boldsymbol{x}\|\,\|\boldsymbol{y}\|$, $\left|\boldsymbol{x}^T\boldsymbol{y}\right| \leq \|\boldsymbol{x}\|\,\|\boldsymbol{y}\|$, $\|\boldsymbol{A}\boldsymbol{x}\| \leq \|\boldsymbol{A}\|\,\|\boldsymbol{x}\|$, then

$$\begin{aligned}\dot{V}_1 &= \boldsymbol{s}^T\dot{\boldsymbol{s}} + \boldsymbol{\varepsilon}^T\dot{\boldsymbol{\varepsilon}} + \dot{\boldsymbol{e}}_0^T\ddot{\boldsymbol{e}}_0 \\ &\leq \Lambda_2\Gamma_2\|\boldsymbol{s}\|\left\|\left|\dot{\boldsymbol{e}}_0\right|^{\Gamma_2-1}\circ\Bigg[\boldsymbol{e}_1^2 + \frac{\partial \boldsymbol{F}(\boldsymbol{x}_1,\boldsymbol{x}_2)}{\partial \boldsymbol{x}_2}\boldsymbol{e}_2^1 \\ &\quad + \frac{\partial \boldsymbol{F}(\boldsymbol{x}_1,\boldsymbol{x}_2)}{\partial \boldsymbol{x}_1}\boldsymbol{e}_1^1\Bigg]\right\| + \|\boldsymbol{s}\|\left\|\left(\boldsymbol{I}_1 + \Lambda_1\Gamma_1\left|\boldsymbol{\varepsilon}\right|^{\Gamma_1-1}\right)\circ\boldsymbol{e}_1^1\right\| \\ &\quad + \|\boldsymbol{\varepsilon}\|\left\|\dot{\boldsymbol{e}}_0 + \boldsymbol{e}_1^1\right\| + \|\dot{\boldsymbol{e}}_0\|\left\|\boldsymbol{e}_1^2 + \frac{\partial \boldsymbol{F}(\boldsymbol{x}_1,\boldsymbol{x}_2)}{\partial \boldsymbol{x}_2}\boldsymbol{e}_2^1\right. \\ &\quad \left. + \frac{\partial \boldsymbol{F}(\boldsymbol{x}_1,\boldsymbol{x}_2)}{\partial \boldsymbol{x}_1}\boldsymbol{e}_1^1\right\| + \|\dot{\boldsymbol{e}}_0\|\left\|M_1\left|\boldsymbol{s}\right|^{\alpha}\circ sgn(\boldsymbol{s}) + M_2\boldsymbol{s}\right\| \\ &\leq \Lambda_2\Gamma_2\|\boldsymbol{s}\|\left\|\left|\dot{\boldsymbol{e}}_0\right|^{\Gamma_2-1}\right\|\left\|\boldsymbol{e}_1^2\right. \\ &\quad \left. + \frac{\partial \boldsymbol{F}(\boldsymbol{x}_1,\boldsymbol{x}_2)}{\partial \boldsymbol{x}_2}\boldsymbol{e}_2^1 + \frac{\partial \boldsymbol{F}(\boldsymbol{x}_1,\boldsymbol{x}_2)}{\partial \boldsymbol{x}_1}\boldsymbol{e}_1^1\right\| \\ &\quad + \|\boldsymbol{s}\|\left\|\boldsymbol{I}_1 + \Lambda_1\Gamma_1\left|\varepsilon\right|^{\Gamma_1-1}\right\|\left\|\boldsymbol{e}_1^1\right\| \\ &\quad + \|\boldsymbol{\varepsilon}\|\left(\|\dot{\boldsymbol{e}}_0\| + \left\|\boldsymbol{e}_1^1\right\|\right) + \|\dot{\boldsymbol{e}}_0\|\left\|\boldsymbol{e}_1^2 + \frac{\partial \boldsymbol{F}(\boldsymbol{x}_1,\boldsymbol{x}_2)}{\partial \boldsymbol{x}_2}\boldsymbol{e}_2^1\right. \\ &\quad \left. + \frac{\partial \boldsymbol{F}(\boldsymbol{x}_1,\boldsymbol{x}_2)}{\partial \boldsymbol{x}_1}\boldsymbol{e}_1^1\right\| + \|\dot{\boldsymbol{e}}_0\|\left(\left\|M_1\left|\boldsymbol{s}\right|^{\alpha}\circ sgn(\boldsymbol{s})\right\| + \|M_2\boldsymbol{s}\|\right)\end{aligned} \tag{47}$$

Moreover, considering that $|a|^l \leq 1 + |a|$ while $0 < l < 1$, the following inequalities can be obtained:

$$\left\|\left|\dot{\boldsymbol{e}}_0\right|^{\Gamma_2-1}\right\| \leq \|\boldsymbol{I}_1 + |\dot{\boldsymbol{e}}_0|\| \leq \|\boldsymbol{I}_1\| + \|\dot{\boldsymbol{e}}_0\| = \sqrt{3} + \|\dot{\boldsymbol{e}}_0\| \tag{48}$$

$$\begin{aligned}&\left\|\boldsymbol{I}_1 + \Lambda_1\Gamma_1\left|\varepsilon\right|^{\Gamma_1-1}\right\| \leq \|\boldsymbol{I}_1 + \Lambda_1\Gamma_1\left(\boldsymbol{I}_1 + |\varepsilon|\right)\| \\ &= \|(1+\Lambda_1\Gamma_1)\boldsymbol{I}_1 + \Lambda_1\Gamma_1|\varepsilon|\| \leq \sqrt{3}\left(1+\Lambda_1\Gamma_1\right) + \Lambda_1\Gamma_1\|\varepsilon\|\end{aligned} \tag{49}$$

$$\begin{aligned}&\left\|M_1\left|\boldsymbol{s}\right|^{\alpha}\circ sgn(\boldsymbol{s})\right\| \leq M_1\left\|\left|\boldsymbol{s}\right|^{\alpha}\right\|\|sgn(\boldsymbol{s})\| \\ &\leq \sqrt{3}M_1\|\boldsymbol{I}_1 + |\boldsymbol{s}|\| \leq \sqrt{3}M_1\left(\sqrt{3} + \|\boldsymbol{s}\|\right)\end{aligned} \tag{50}$$

Then Equ. 47 is further transformed as follows:

$$\begin{aligned}\dot{V}_1 &= \boldsymbol{s}^T\dot{\boldsymbol{s}} + \boldsymbol{\varepsilon}^T\dot{\boldsymbol{\varepsilon}} + \dot{\boldsymbol{e}}_0^T\ddot{\boldsymbol{e}}_0 \\ &\leq \Lambda_2\Gamma_2\|\boldsymbol{s}\|\left(\sqrt{3} + \|\dot{\boldsymbol{e}}_0\|\right)\left\|\boldsymbol{e}_1^2\right. \\ &\quad \left. + \frac{\partial \boldsymbol{F}(\boldsymbol{x}_1,\boldsymbol{x}_2)}{\partial \boldsymbol{x}_2}\boldsymbol{e}_2^1 + \frac{\partial \boldsymbol{F}(\boldsymbol{x}_1,\boldsymbol{x}_2)}{\partial \boldsymbol{x}_1}\boldsymbol{e}_1^1\right\| \\ &\quad + \|\boldsymbol{s}\|\left(\sqrt{3}\left(1 + \Lambda_1\Gamma_1\right) + \Lambda_1\Gamma_1\|\boldsymbol{\varepsilon}\|\right)\left\|\boldsymbol{e}_1^1\right\| \\ &\quad + \|\boldsymbol{\varepsilon}\|\left(\|\dot{\boldsymbol{e}}_0\| + \left\|\boldsymbol{e}_1^1\right\|\right) + \|\dot{\boldsymbol{e}}_0\|\left\|\boldsymbol{e}_1^2 + \frac{\partial \boldsymbol{F}(\boldsymbol{x}_1,\boldsymbol{x}_2)}{\partial \boldsymbol{x}_2}\boldsymbol{e}_2^1\right. \\ &\quad \left. + \frac{\partial \boldsymbol{F}(\boldsymbol{x}_1,\boldsymbol{x}_2)}{\partial \boldsymbol{x}_1}\boldsymbol{e}_1^1\right\| + \|\dot{\boldsymbol{e}}_0\|\left(\sqrt{3}M_1\left(\sqrt{3} + \|\boldsymbol{s}\|\right) + \|M_2\boldsymbol{s}\|\right) \\ &\leq \left(\sqrt{3}\Lambda_2\Gamma_2\|\boldsymbol{s}\| + \Lambda_2\Gamma_2\left(\frac{\|\boldsymbol{s}\|^2 + \|\dot{\boldsymbol{e}}_0\|^2}{2}\right)\right) \\ &\quad \left\|\boldsymbol{e}_1^2 + \frac{\partial \boldsymbol{F}(\boldsymbol{x}_1,\boldsymbol{x}_2)}{\partial \boldsymbol{x}_2}\boldsymbol{e}_2^1 + \frac{\partial \boldsymbol{F}(\boldsymbol{x}_1,\boldsymbol{x}_2)}{\partial \boldsymbol{x}_1}\boldsymbol{e}_1^1\right\| \\ &\quad + \sqrt{3}\left(1 + \Lambda_1\Gamma_1\right)\|\boldsymbol{s}\|\left\|\boldsymbol{e}_1^1\right\| \\ &\quad + \Lambda_1\Gamma_1\left(\frac{\|\dot{\boldsymbol{e}}_0\|^2 + \|\boldsymbol{s}\|^2}{2}\right)\left\|\boldsymbol{e}_1^1\right\| + \left(\frac{\|\boldsymbol{\varepsilon}\|^2 + \|\dot{\boldsymbol{e}}_0\|^2}{2}\right) \\ &\quad + \|\boldsymbol{\varepsilon}\|\left\|\boldsymbol{e}_1^1\right\| + \|\dot{\boldsymbol{e}}_0\|\left\|\boldsymbol{e}_1^2 + \frac{\partial \boldsymbol{F}(\boldsymbol{x}_1,\boldsymbol{x}_2)}{\partial \boldsymbol{x}_2}\boldsymbol{e}_2^1 + \frac{\partial \boldsymbol{F}(\boldsymbol{x}_1,\boldsymbol{x}_2)}{\partial \boldsymbol{x}_1}\boldsymbol{e}_1^1\right\| \\ &\quad + 3M_1\|\dot{\boldsymbol{e}}_0\| + \sqrt{3}M_1\left(\frac{\|\dot{\boldsymbol{e}}_0\|^2 + \|\boldsymbol{s}\|^2}{2}\right) \\ &\quad + M_2\left(\frac{\|\dot{\boldsymbol{e}}_0\|^2 + \|\boldsymbol{s}\|^2}{2}\right) \\ &\leq \left(\sqrt{3}\Lambda_2\Gamma_2\left(\frac{1 + \|\boldsymbol{s}\|^2}{2}\right) + \Lambda_2\Gamma_2\left(\frac{\|\boldsymbol{s}\|^2 + \|\dot{\boldsymbol{e}}_0\|^2}{2}\right)\right) \\ &\quad \left\|\boldsymbol{e}_1^2 + \frac{\partial \boldsymbol{F}(\boldsymbol{x}_1,\boldsymbol{x}_2)}{\partial \boldsymbol{x}_2}\boldsymbol{e}_2^1 + \frac{\partial \boldsymbol{F}(\boldsymbol{x}_1,\boldsymbol{x}_2)}{\partial \boldsymbol{x}_1}\boldsymbol{e}_1^1\right\| \\ &\quad + \sqrt{3}\left(1 + \Lambda_1\Gamma_1\right)\left(\frac{1 + \|\boldsymbol{s}\|^2}{2}\right)\left\|\boldsymbol{e}_1^1\right\|\end{aligned}$$

$$
\begin{aligned}
&+\Lambda_1\Gamma_1\left(\frac{\|\dot{\boldsymbol{\varepsilon}}_0\|^2+\|\boldsymbol{s}\|^2}{2}\right)\left\|\boldsymbol{e}_1^1\right\|+\left(\frac{\|\boldsymbol{\varepsilon}\|^2+\|\dot{\boldsymbol{\varepsilon}}_0\|^2}{2}\right)\\
&+\left(\frac{1+\|\boldsymbol{\varepsilon}\|^2}{2}\right)\left\|\boldsymbol{e}_1^1\right\|+\left(\frac{1+\|\dot{\boldsymbol{\varepsilon}}_0\|^2}{2}\right)\left\|\boldsymbol{e}_1^2\right.\\
&\left.+\frac{\partial \boldsymbol{F}(\boldsymbol{x}_1,\boldsymbol{x}_2)}{\partial \boldsymbol{x}_2}\boldsymbol{e}_2^1+\frac{\partial \boldsymbol{F}(\boldsymbol{x}_1,\boldsymbol{x}_2)}{\partial \boldsymbol{x}_1}\boldsymbol{e}_1^1\right\|\\
&+3M_1\left(\frac{1+\|\dot{\boldsymbol{\varepsilon}}_0\|^2}{2}\right)+\sqrt{3}M_1\left(\frac{\|\dot{\boldsymbol{\varepsilon}}_0\|^2+\|\boldsymbol{s}\|^2}{2}\right)\\
&+M_2\left(\frac{\|\dot{\boldsymbol{\varepsilon}}_0\|^2+\|\boldsymbol{s}\|^2}{2}\right)\\
&\leq K_V V_1+K_L
\end{aligned}
\tag{51}
$$

where $K_V = \max\{k_1, k_2\}$, $K_L = \max_t\{(1+\sqrt{3}\Lambda_2\Gamma_2)\left\|\boldsymbol{e}_1^2+\frac{\partial \boldsymbol{F}(\boldsymbol{x}_1,\boldsymbol{x}_2)}{\partial \boldsymbol{x}_2}\boldsymbol{e}_2^1+\frac{\partial \boldsymbol{F}(\boldsymbol{x}_1,\boldsymbol{x}_2)}{\partial \boldsymbol{x}_1}\boldsymbol{e}_1^1\right\|+(1+\sqrt{3}(1+\Lambda_1\Gamma_1))\left\|\boldsymbol{e}_1^1\right\|+3M_1\}$,
$k_1=\max_t\{(\sqrt{3}+1)\Lambda_2\Gamma_2\left\|\boldsymbol{e}_1^2+\frac{\partial \boldsymbol{F}(\boldsymbol{x}_1,\boldsymbol{x}_2)}{\partial \boldsymbol{x}_2}\boldsymbol{e}_2^1+\frac{\partial \boldsymbol{F}(\boldsymbol{x}_1,\boldsymbol{x}_2)}{\partial \boldsymbol{x}_1}\boldsymbol{e}_1^1\right\|+(\Lambda_1\Gamma_1+\sqrt{3}(1+\Lambda_1\Gamma_1))\left\|\boldsymbol{e}_1^1\right\|+\sqrt{3}M_1+M_2\}$,
$k_2\max_t\{(1+\Lambda_2\Gamma_2)\left\|\boldsymbol{e}_1^2+\frac{\partial \boldsymbol{F}(\boldsymbol{x}_1,\boldsymbol{x}_2)}{\partial \boldsymbol{x}_2}\boldsymbol{e}_2^1+\frac{\partial \boldsymbol{F}(\boldsymbol{x}_1,\boldsymbol{x}_2)}{\partial \boldsymbol{x}_1}\boldsymbol{e}_1^1\right\|+\Lambda_1\Gamma_1\left\|\boldsymbol{e}_1^1\right\|+(3+\sqrt{3})M_1+M_2+1\}$.

It can be concluded that Lyapunov function V_1 is finite-time bounded.

REFERENCES

[1] E. B. Jackson and C. W. Buttrill, "Control laws for a wind tunnel free-flight study of a blended-wing-body aircraft," Langley Res. Center, Hampton, VI, USA, Tech. Rep. TM-2006-214501, Aug. 2006.

[2] G. Stenfelt and U. Ringertz, "Lateral stability and control of a tailless aircraft configuration," *J. Aircr.*, vol. 46, no. 6, pp. 2161–2164, Nov. 2009.

[3] G. Stenfelt and U. Ringertz, "Yaw control of a tailless aircraft configuration," *J. Aircr.*, vol. 47, no. 5, pp. 1807–1811, Sep./Oct. 2010.

[4] M. Zak, "Terminal attractors for addressable memory in neural networks," *Phys. Lett. A*, vol. 133, nos. 1–2, pp. 18–22, 1988.

[5] Y. Feng, X. Yu, and Z. Man, "Non-singular terminal sliding mode control of rigid manipulators," *Automatica*, vol. 38, no. 12, pp. 2159–2167, 2002.

[6] L. Yang and J. Yang, "Nonsingular fast terminal sliding-mode control for nonlinear dynamical systems," *Int. J. Robust Nonlinear Control*, vol. 21, no. 16, pp. 1865–1879, Nov. 2011.

[7] A. Polyakov, "Nonlinear feedback design for fixed-time stabilization of linear control systems," *IEEE Trans. Autom. Control*, vol. 57, no. 8, pp. 2106–2110, Aug. 2012.

[8] H. H. Choi, "Variable structure output feedback control design for a class of uncertain dynamic systems," *Automatica*, vol. 38, no. 2, pp. 335–341, Feb. 2002.

[9] K.-S. Kim, Y. Park, and S.-H. Oh, "Designing robust sliding hyperplanes for parametric uncertain systems: A Riccati approach," *Automatica*, vol. 36, no. 7, pp. 1041–1048, Jul. 2000.

[10] Y. Chang, "Adaptive sliding mode control of multi-input nonlinear systems with perturbations to achieve asymptotical stability," *IEEE Trans. Autom. Control*, vol. 52, no. 12, pp. 2863–2869, Dec. 2009.

[11] W.-J. Cao and J.-X. Xu, "Nonlinear integral-type sliding surface for both matched and unmatched uncertain systems," *IEEE Trans. Autom. Control*, vol. 49, no. 8, pp. 1355–1360, Aug. 2004.

[12] J. Yang, S. Li, C. Sun, and L. Guo, "Nonlinear-disturbance-observer-based robust flight control for airbreathing hypersonic vehicles," *IEEE Trans. Aerosp. Electron. Syst.*, vol. 49, no. 2, pp. 1263–1275, Apr. 2013.

[13] D. Ginoya, P. D. Shendge, and S. B. Phadke, "Sliding mode control for mismatched uncertain systems using an extended disturbance observer," *IEEE Trans. Ind. Electron.*, vol. 61, no. 4, pp. 1983–1992, Apr. 2014.

[14] Y. B. Shtessel, I. A. Shkolnikov, and A. Levant, "Smooth second-order sliding modes: Missile guidance application," *Automatica*, vol. 43, no. 8, pp. 1470–1476, Aug. 2007.

[15] E. Cruz-Zavala, J. A. Moreno, and L. M. Fridman, "Uniform robust exact differentiator," *IEEE Trans. Autom. Control*, vol. 56, no. 11, pp. 2727–2733, Nov. 2011.

[16] M. Basin, P. Yu, and Y. Shtessel, "Finite- and fixed-time differentiators utilising HOSM techniques," *IET Control Theory Appl.*, vol. 11, no. 8, pp. 1144–1152, May 2017.

[17] J. Yang, S. Li, J. Su, and X. Yu, "Continuous nonsingular terminal sliding mode control for systems with mismatched disturbances," *Automatica*, vol. 49, no. 7, pp. 2287–2291, 2013.

[18] J. Yang, S. Li, and X. Yu, "Sliding-mode control for systems with mismatched uncertainties via a disturbance observer," *IEEE Trans. Ind. Electron.*, vol. 60, no. 1, pp. 160–169, Jan. 2013.

[19] J. Yang, J. Su, S. Li, and X. Yu, "High-order mismatched disturbance compensation for motion control systems via a continuous dynamic sliding-mode approach," *IEEE Trans. Ind. Informat.*, vol. 10, no. 1, pp. 604–614, Feb. 2014.

[20] J. Zhang, X. Liu, Y. Xia, Z. Zuo, and Y. Wang, "Disturbance observer-based integral sliding-mode control for systems with mismatched disturbances," *IEEE Trans. Ind. Electron.*, vol. 63, no. 11, pp. 7040–7048, Nov. 2016.

[21] X. Fang and F. Liu, "High-order mismatched disturbance rejection control for small-scale unmanned helicopter via continuous nonsingular terminal sliding-mode approach," *Int. J. Robust Nonlinear Control*, vol. 29, pp. 935–948, Mar. 2019.

[22] R. Su, Q. Zong, B. Tian, and M. You, "Comprehensive design of disturbance observer and non-singular terminal sliding mode control for reusable launch vehicles," *IET Control Theory Appl.*, vol. 9, no. 12, pp. 1821–1830, Aug. 2015.

[23] D. Q. Mayne, J. B. Rawlings, C. V. Rao, and P. O. M. Scokaert, "Constrained model predictive control: Stability and optimality," *Automatica*, vol. 36, no. 6, pp. 789–814, 2000.

[24] E. Gilbert and I. Kolmanovsky, "Nonlinear tracking control in the presence of state and control constraints: A generalized reference governor," *Automatica*, vol. 38, no. 12, pp. 2063–2073, 2002.

[25] K. B. Ngo, R. Mahony, and Z.-P. Jiang, "Integrator backstepping using barrier functions for systems with multiple state constraints," in *Proc. 44th IEEE Conf. Decis. Control*, Seville, Spain, Dec. 2005, pp. 8306–8312.

[26] K. P. Tee, S. S. Ge, and E. H. Tay, "Barrier Lyapunov functions for the control of output-constrained nonlinear systems," *Automatica*, vol. 45, no. 4, pp. 918–927, Apr. 2009.

[27] K. P. Tee and S. S. Ge, "Control of nonlinear systems with partial state constraints using a barrier Lyapunov function," *Int. J. Control*, vol. 84, no. 12, pp. 2008–2023, 2011.

[28] Z. Wang, Y. Sun, and B. Liang, "Synchronization control for bilateral teleoperation system with position error constraints: A fixed-time approach," *ISA Trans.*, vol. 93, pp. 125–136, Oct. 2019, doi: 10.1016/J.ISATRA.2019.03.003.

[29] L. Qiao and W. Zhang, "Adaptive non-singular integral terminal sliding mode tracking control for autonomous underwater vehicles," *IET Control Theory Appl.*, vol. 11, no. 8, pp. 1293–1306, Feb. 2017.

[30] L. Qiao and W. Zhang, "Double-loop integral terminal sliding mode tracking control for UUVs with adaptive dynamic compensation of uncertainties and disturbances," *IEEE J. Ocean. Eng.*, vol. 44, no. 1, pp. 29–53, Jan. 2019.

[31] J. Sun, J. Yi, Z. Pu, and X. Tan, "Fixed-time sliding mode disturbance observer-based nonsmooth backstepping control for hypersonic vehicles," *IEEE Trans. Syst., Man, Cybern., Syst.*, to be published, doi: 10.1109/TSMC.2018.2847706.

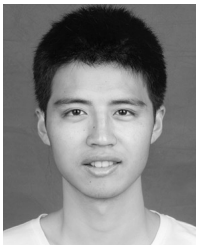

ZHIRUN CHEN received the B.E. degree in detection, guidance and control technology from the Nanjing University of Aeronautics and Astronautics, Nanjing, China, in 2017. He is currently pursuing the master's degree with the Department of Automation, Tsinghua University, Beijing, China.

His research interests include sliding mode control and barrier Lyapunov function.

QING LI received the bachelor's, master's, and Ph.D. degrees from the Nanjing University of Aeronautics and Astronautics.

He is currently a Professor with the Department of Automation, Tsinghua University, China, where he has taught, since 2000, with major research interests in system architecture, enterprise modeling, and system performance evaluation. He has published six books and more than 200 articles in esteemed magazines and conferences in China and abroad.

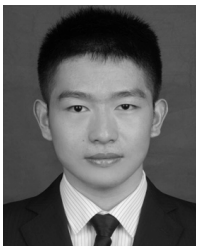

XIAOZHE JU received the B.S. degree in detection, guidance and control technology from the Nanjing University of Aeronautics and Astronautics, Nanjing, China, in 2016. He is currently pursuing the Ph.D. degree with the School of Astronautics, Harbin Institute of Technology, Harbin, China.

His research interests include guidance and control of advanced vehicles, robust control theory, and sliding mode control theory.

FEI CEN received the B.S. degree in automation from Tsinghua University, in 2008, and the M.S. degree in aircraft design from the China Aerodynamics Research and Development Center, in 2011. He is currently pursuing the Ph.D. degree in control theory and control engineering with Tsinghua University.

His research interests include unsteady aerodynamics modeling, nonlinear flight dynamics, and flight control under extremely conditions.